BASIC TRANSLOCATION UNIT COMPOSITION OF THE TWIN ARGININE TRANSLOCASE (TAT) SYSTEM IN PEA THYLAKOIDS

By

JOSE MIGUEL CELEDON

A DISSERTATION PRESENTED TO THE GRADUATE SCHOOL
OF THE UNIVERSITY OF FLORIDA IN PARTIAL FULFILLMENT
OF THE REQUIREMENTS FOR THE DEGREE OF
DOCTOR OF PHILOSOPHY

UNIVERSITY OF FLORIDA

2011

© 2011 Jose Miguel Celedon

To my family and teachers

ACKNOWLEDGMENTS

I would like to thank my advisor and mentor, Dr. Kenneth Cline, and the members of my graduate committee, Drs.: Mark Settles, Brian Cain, Curt Hannah, and Kevin Folta, for their support, advice and encouragement. I would also like to thank Dr. Steve Theg from University of California, Davis, for his insightful comments and contributions to the analysis and interpretation of kinetic data. I would like to specially thank the members of Dr. Cline's lab, Dr. Cassie Aldridge, Dr. Ma Xianyue, Dr. Carole Dabney-Smith, Dr. Jonathan Martin, and Mike McCaffery, whom have all helped me with their experience and with whom I had many fruitful discussions. I would also like to acknowledge Dr. Sixue Chen and Carolyn Diaz from the Interdisciplinary Center for Biotechnology Research, Mass Spectrometry lab, for lending their assistance and help.

TABLE OF CONTENTS

page

LIST OF TABLES

LIST OF FIGURES

LIST OF ABBREVIATIONS

Alb3	Albino 3, membrane protein insertase machinery of chloroplast thylakoids
ATP	Adenosine triphosphate
BN	Blue native
Chl	Chlorophyll
Cp	Chloroplast
cpTat	Twin arginine protein translocase of chloroplast thylakoids
cpTatC	Subunit C of the cpTat translocase
Cys	Cysteine
DNA	Deoxyribonucleic acid
dpm	Disintegrations per minute
DTT	Dithiothreitol
EM	Electron microscopy
GTP	Guanosine triosphosphate
h	Hour, time
Hcf106	High chlorophyll fluorescence 106, a membrane-integrated subunit of the cpTat translocase
HK	10 mM HEPES-KOH pH 8.0, buffer used to hypotonically lyse isolated chloroplasts *in vitro*
IB	Import buffer
IP	Immunoprecipitation
kDa	Kilodalton
-M	Molar concentration
m-	Mature processed form of a translocated protein
µg	Microgram of mass

min	Minutes, time
mL	Milliliter of volume
µL	Microliter of volume
mM	Millimolar concentration
µM	Micromolar concentration
Mr	Relative molecular weight markers
mRNA	Messenger ribonucleic acid
OE-	Oxygen evolving complex
Oxa1	Oxidase assembly machinery of mitochondria
P	Pellet
-PAGE	Polyacrylamide gel electrophoresis
PCR	Polymerase chain reaction
PMF	Proton motive force
PMSF	Phenylmethanesulfonyl fluoride
pre-	Precursor for of a protein in question
ps-	*Pisum sativum* antibodies
SAM	Sorting and assembly machinery of mitochondria
SDS-	Sodium dodecyl sulfate, protein denaturing detergent
Sec	Secretory protein translocase
SN	Supernatant
SPP	Stromal processing peptidase of chloroplast
SP6	Phage DNA dependent RNA polymerase that is used to synthesize mRNA *in vitro*
+T	Chloroplast membrane fraction that has been treated with thermolysin protease
TBS	Tris-buffered saline solution

Th	Thermolysin protease
Tha4	Thylakoid assembly 4, membrane-integrated subunit of the cpTat protein translocase
Thy	Thylakoids
Tic	Translocon of the inner envelope of chloroplast
Tim	Translocon of the inner membrane of mitochondria
Toc	Translocon of the outer envelope of chloroplast
Tom	Translocon of the outer membrane of mitochondria
TM	Transmembrane
Tp	Translation product
WG	Wheat germ
YidC	Membrane protein insertase machinery of *E coli*

Abstract of Dissertation Presented to the Graduate School
of the University of Florida in Partial Fulfillment of the
Requirements for the Degree of Doctor of Philosophy

BASIC TRANSLOCATION UNIT COMPOSITION OF THE TWIN ARGININE TRANSLOCASE (TAT) SYSTEM IN PEA THYLAKOIDS

By

Jose Miguel Celedon

August 2011

Chair: Kenneth C. Cline
Major: Horticultural Science

Tat (twin arginine translocation) systems transport proteins in folded conformation across prokaryote and prokaryote-derived membranes without breaching the permeability barrier. The machinery consists of three components in the photosynthetic thylakoid membrane. Multiple copies of Hcf106 and cpTatC form a receptor complex that recognizes the twin arginine signal peptide of precursor proteins. cpTatC is the primary receptor component. After precursor proteins bind to the receptor complex, Tha4, thought to facilitate transmembrane passage, assembles as a homo-oligomer with the precursor bound receptor complex and the precursor protein is transported across the membrane.

Here, we used saturation binding analysis of the OE17 precursor and transport kinetics to determine the stoichiometry of Tat components for binding and transport. For these studies we developed a novel quantitative immunoblotting method that uses radiolabeled full-length proteins as standards of known concentration to quantify endogenous Tat components with an error of 5-8%. Three separate approaches showed that each cpTatC non-cooperatively binds a precursor protein, suggesting that a fully occupied receptor complex binds 8 precursor proteins. Transport kinetics of

bound precursor showed that precursor-bound sites are independently functional for transport and that, with sufficient Tha4, the translocation step obeys first order kinetics with a k_{cat} ~0.3 min^{-1}. Analysis of transport rate as a function of the Tha4 concentration identified a breakpoint in the relationship, indicating that 28 Tha4 protomers is the minimal oligomer for transport of a single OE17 precursor protein. These results offer insight into the yet undetermined translocation mechanism of the Tat system and a means to test current hypotheses for the transmembrane passage of precursor proteins.

CHAPTER 1
PROTEIN TRANSPORT ACROSS BIOLOGICAL MEMBRANES AND THE MECHANISTIC ROLE OF OLIGOMER FORMATION

Overview

Our understanding of protein translocation systems has deeply changed in the last decade. Crystal structures and elegant biochemical studies of protein transport in organelles, the endoplasmic reticulum (ER) and the cytoplasmic membrane of prokaryotes are unraveling an unexpected level of complexity and sophistication in the targeting and localization of proteins. Emerging evidence from different protein transport systems suggests that homo-oligomers play different roles in the molecular machineries that constitute the active translocases. In some cases, oligomers provide docking platforms that stabilize interactions playing an indirect function during translocation. In other instances, homo-oligomeric assemblies have been proposed as the mechanism for transient pore formation, playing a key role in protein transport. Other functions could also arise for homo-oligomers in protein transport. For example, in other systems not related to protein translocation, homo-oligomers allow allosteric cooperativity and provide multivalent active sites in enzymes among other functions. Here, we will review the current knowledge about the role of homo-oligomeric assemblies in protein transport systems and its implications in the mechanisms of protein translocation.

Introduction

Protein targeting and localization have been essential features of life since membranes appeared as the boundary defining elements that created different subcellular compartments. The new barriers imposed by membranes allowed cells to modify and optimize each compartment for specific functions and metabolic reactions. This process of compartment specialization most likely occurred in parallel to the

development of membrane protein insertion systems (Bohnsack and Schleiff, 2010). Proteins spanning the membrane bilayer were necessary to control the concentration and composition of each compartment and allowed the communication between them and the external environment. Phylogenetic and bioinformatic studies suggest that membrane transporters arose from small peptides consisting of single and double transmembrane domains (TM) that could oligomerize to create structures able to transport small molecules across the membrane (Saier, 2003). These peptides probably inserted “spontaneously” into the lipid bilayer through their hydrophobic TM domains, giving rise to the first targeting signals in the primordial cell (Blobel et al., 1980; Pohlschröder et al., 2005). Later in evolution, intragenic duplication events allowed small molecule transporters to evolve into larger and more complex structures that had soluble domains to interact specifically with substrates or other proteins (Saier, 2000). This enabled a new variety of functions in membrane transporters that ultimately gave rise to the protein translocation machineries we find in modern day prokaryotes and eukaryotes (Pohlschröder et al., 2005).

Sec Protein Transport

Sec systems are universally conserved and constitute the major route for protein insertion and secretion in the cell. The Sec channel is a heterotrimer complex formed by Sec61$\alpha\beta\gamma$ in eukaryotes and SecYEG in bacteria. The Sec61α subunit in eukaryotes and SecY in bacteria form the Sec channel, an hourglass shaped channel through which proteins are threaded in an unfolded conformation (Rapoport, 2007). The Sec channel is a central but passive component that requires the interaction with other partners for transport of proteins across or into the membrane. Some of these interactions result in Sec-channel oligomers that provide specific functions.

During cotranslational transport the Sec channel associates with ribosomes to translocate proteins as they are translated and emerge from the ribosome. This mode of translocation is especially important for integral membrane proteins that are more likely to aggregate if released in a hydrophilic environment. In cotranslational transport the signal peptide is recognized by SRP as it emerges from the ribosome (Luirink and Sinning, 2004). Upon SRP binding, translation halts until the SRP-ribosome complex docks with the SRP receptor in the membrane (Gilmore et al., 1982). After this, the ribosome is transferred to a Sec channel, translation resumes and TM domains are laterally released into the lipid bilayer (Rapoport, 2007). At some point in the process that is not yet clear, the ribosome-Sec channel complex associates with three other unoccupied Sec channels forming a tetramer that can be visualized by electron cryo-microscopy of arrested translating ribosomes (Ménétret et al., 2005; Osborne et al., 2005). In this oligomeric arrangement, it is thought that only one Sec channel serves to translocate the preprotein and the others participate in the interactions with the ribosome, possibly providing more stability to the complex.

Oligomers of Sec channels also seem to play an important role in posttranslational transport. In this mode of transport, preproteins are kept in a transport competent conformation by chaperones and directed to the Sec channel. In bacteria, binding of the ATPase SecA to the preprotein and association with the SecYEG translocase promotes cycles of ATP hydrolysis that drive protein transport (Economou and Wickner, 1994). It has been proposed that precursor translocation by SecA occurs by a pushing mechanism, in which SecA ATP driven conformational changes result in binding and release of the precursor and vectorial movement through the Sec channel (Rapoport,

2007). Evidence of Sec channel oligomers in posttranslational transport comes from crosslinking studies in bacteria where two SecY copies were fused in tandem with one copy carrying an inactivating mutation that could be rescued with a WT SecY second copy (Osborne and Rapoport, 2007). Interestingly, the rescued SecY could be crosslinked to the signal peptide and mature domain of the preprotein and the WT copy to SecA indicating that only one copy serves as the channel while the other serves as a docking platform for SecA. In eukaryotes, posttranslational transport occurs by a ratcheting mechanism where BiP, an ER lumen ATPase, is recruited to the Sec channel and binds to the incoming preprotein in the trans side of the membrane (Panzner et al., 1995). In this mode of transport, the preprotein is thought to move through the channel by Brownian motion and BiP binding would prevent backsliding and allow a net forward movement into the ER (Rapoport, 2007). Although, no direct evidence for Sec channel oligomers has been found in posttranslational translocation in eukaryotes, it is conceivable that a similar mechanism is in place for BiP docking and binding to the incoming preprotein.

Organelle Protein Import Systems

Organelles are eukaryotic inventions that play different fundamental roles in the cell's metabolism. They are characterized for being membrane enclosed internal compartments in the cell, and therefore require protein translocation systems to correctly localize their protein complement. For the endomembrane system organelles and the peroxisomes, this is at least partially accomplished by trafficking of vesicles that contain proteins integrated into their membranes or cargo proteins that have been translocated by the Sec system into the ER (Pfeffer and Rothman, 1987). In this way,

the Sec translocase and a complex protein and vesicle sorting system directly participate in the biogenesis and maintenance of these organelles.

Prokaryotic derived organelles, namely mitochondria and plastids, retain a functional genetic system and translation machineries. However, ~99% of the protein coding genes were transferred to the host nucleus, and thus require relocation to their original compartments (Wickner and Schekman, 2005). Vesicle transport was not an ideal system for these organelles since simple vesicle fusion would not directly allow access to the inner compartments of these organelles (Gross and Bhattacharya, 2009). To address this issue, eukaryotic cells developed new protein transport systems that are able to target newly synthesized proteins to all subcompartments of prokaryote derived organelles.

Mitochondrial Protein Import Systems

Proteins encoded in the nucleus and translated on cytosolic ribosomes are targeted to the mitochondrial surface by two classes or targeting signals: N-terminal cleavable signals or discrete internal signals distributed along the mature domain of the protein (Dolezal et al., 2006; Neupert and Herrmann, 2007). The first step in protein import into mitochondria is mediated by the Translocase of the Outer Membrane (Tom) complex. The Tom complex is composed of several membrane proteins that can be divided in two groups according to their function: receptors and channel-forming proteins. The receptors Tom20 and Tom70, specialize in recognizing preproteins containing N-terminal cleavable presequences or internal targeting sequences respectively (Neupert and Herrmann, 2007). The central component that forms the Tom channel is Tom40, which is predicted to have a β-barrel structure. Interestingly, individual Tom40 channels appear to form dimers as suggested by single particle

imaging of solubilized complexes (Kunkele et al., 1998). Based on the molecular weight of the Tom complex, it was suggested that each Tom channel contains more than one copy of Tom40 (Kunkele et al., 1998), hence oligomerization of Tom40 molecules plays a dual role in the biogenesis of the Tom complex, i.e. in the formation of individual Tom channels and in the assembly of the active Tom complex with two Tom channels. Dimers or trimers of porins and channels in the outer membrane of prokaryotes and prokaryote-derived organelles are not rare but is surprising that Tom40 developed this ability considering it is a β-barrel of eukaryotic origin (Dyall et al., 2004). After receptor binding, preproteins are released from cytosolic chaperones and cross the Tom channel by walking through a sequence of binding sites with increasing affinity along the channel (Komiya et al., 1998). It is still not clear if Tom channels can be active simultaneously or if, as in Sec channel dimers, only one copy is active while the other plays a complementary role during translocation.

After crossing the outer membrane, preproteins destined to the mitochondrial matrix and the inner membrane associate with the receptors of the Tim23 translocase of the inner membrane, Tim23 and Tim50 (Chacinska et al., 2009; Dolezal et al., 2006; Neupert and Herrmann, 2007). The Tim23 complex contains equimolar amounts of three proteins: Tim23, Tim17 and Tim44 (Moro et al., 1999) two of which have been shown to form dimers. Tim23 transiently forms dimers through the N-terminal receptor domain that is exposed to the inter membrane space (Bauer et al., 1996). Dimer formation requires the membrane electric potential and presequence recognition causes Tim23 dimers to dissociate and to presumably open the channel (Bauer et al., 1996). The C-terminal domain of Tim23 was shown to form channels when reconstituted into

lipid bilayers (Truscott et al., 2001); whether Tim23 also dimerizes to form the channel hasn't been directly demonstrated. In the matrix side of the inner membrane, Tim44 also forms dimers. Tim44 is a peripheral membrane protein that recruits mtHsp70, an ATPase that is a key component of the import motor in the Tim23 complex. Dimers of Tim44 provide a double docking platform for two mtHsp70 proteins to allow efficient transport of preproteins by a ratcheting mechanism similar to BiP in the ER (Moro et al., 1999). To complete transport, the protein Mge1 triggers the exchange of ADP by ATP in mtHsp70 and the release of the preprotein in the matrix were the presequence is cleaved by the matrix processing peptidase (Gakh et al., 2002). Alternatively, preproteins destined to the inner membrane can be laterally released and integrated by a stop transfer mechanism (van Loon et al., 1986).

Two other pathways can localize preproteins to the inner membrane of mitochondria. In the conservative pathway the bacterially conserved oxidase assembly (Oxa1) machinery allows membrane insertion of preproteins that were fully translocated into the matrix (Hartl et al., 1986). Oxa1 has 5 predicted TM domains and it is proposed to form the core of the translocase. Interestingly, Oxa1 proteins have been shown to form homo-dimers that can cotranslationally integrate inner membrane proteins encoded in the mitochondrial genome (Hell et al., 2001; Kohler et al., 2009). The interactions between Oxa1 dimers and the ribosome show significant parallels to the SecYEG system, presumably with similar mechanistic implications. Alternatively, preproteins lacking a presequence can be directly transferred from the Tom complex to a different inner membrane translocase, the Tim22 complex, which is specialized in integration of solute carrier proteins (Neupert and Herrmann, 2007). In this pathway, a

group of small Tim proteins are essential to prevent aggregation of carrier proteins while they are in the intermembrane space (Webb et al., 2006). The Tim22 complex was reconstituted into planar lipid bilayers after affinity purification and showed conductances characteristic of two coupled pores (Rehling et al., 2003). The two pore structure was confirmed by single-particle electron microscopy (Rehling et al., 2003). Upon incubation of reconstituted Tim22 complex with P2 peptide from the phosphate carrier, one of the channels showed rapid gating activity while the other was closed. From these results it was proposed that the Tim22 complex is composed of two channels that coordinately open and close, one at a time, to integrate carrier proteins into the inner membrane.

The outer membrane of the mitochondrion is derived from its prokaryotic ancestor and most of its proteins have a β-barrel structure. β-barrel membrane proteins are translated in the cytosol, transported through the Tom complex and inserted into the outer membrane with assistance of the sorting and assembly machinery, the Sam complex (Wiedemann et al., 2003). The core component of the Sam complex is Sam50, which has a predicted β-barrel structure and the ability to form channels when reconstituted into lipid bilayers (Paschen et al., 2003). The oligomeric state of Sam50 is unknown but its bacterial homolog, Omp85, was shown to form ring shaped particles in liposomes that when analyzed by BN-PAGE appear as dimers, trimers and possibly tetramers (Robert et al., 2006). The mechanism of β-barrel protein insertion and assembly in the mitochondrial and bacterial outer membrane remains largely unknown. It has been suggested that unfolded preproteins bind to the POTRA domains of Omp85 by β-strand augmentation and that insertion into the membrane occurs at the interface

of Omp85 with the membrane (Hagan et al., 2010).The role of oligomeric assemblies in β-barrel membrane protein insertion remains to be elucidated.

Chloroplasts Protein Import Systems

Access of precursor proteins to the chloroplast is facilitated by the translocases of the outer and inner envelopes, Toc and Tic, respectively (Kouranov et al., 1998; Schnell et al., 1994). Targeting signals, called transit peptides, efficiently direct cytosolic precursor proteins to the chloroplast despite their variability in length and primary sequence (Li and Chiu, 2010). Two receptor components, Toc159 and Toc34 collaborate in the recognition and delivery of precursor proteins to the Toc75 channel. The exact roles of the two receptors are still a matter of debate, however, evidence from different studies suggest that Toc159 provides the initial recognition site and Toc34 facilitates the transfer of the precursor to the channel and translocation across the outer envelope in a GTP hydrolysis dependent manner (Kessler et al., 1994; Schleiff and Becker, 2010; Young et al., 1999). Toc75, a chloroplast homolog of Omp85 in bacteria, can be reconstituted into planar lipid bilayers and displays conductance characteristics of a single pore (Hinnah et al., 1997; Hinnah et al., 2002). Similar to its bacterial homolog, Toc75 has a predicted β-barrel structure as indicated by circular dichroism-spectroscopy, topology studies and prediction programs (Hinnah et al., 1997; Sveshnikova et al., 2000). Despite the electro-physiological evidence of Toc75 forming a single pore channel, the oligomeric state and the organization of the Toc complex and in particular of Toc75, remain controversial. BN-PAGE and size exclusion chromatography suggested that the stoichiometry and composition of the Toc complex is 1:3:3 (Toc159:Toc75:Toc34) (Kikuchi et al., 2006). On the other hand, single particle EM reconstructions of purified Toc complexes show a larger ring with an internal finger-

like structure that divides it into four equal regions (Schleiff et al., 2003). The resolution of the reconstruction is not sufficient to distinguish between 4 individual Toc75 channels or one channel composed of 4 Toc75 proteins. Interestingly, the reconstituted Toc complex was able to bind 4 nanogold-labeled transit peptides in a GTP dependent manner, favoring the idea of a Toc complex with 4 independent channels (Schleiff et al., 2003).

Import of precursor proteins into the chloroplast stroma requires the coordinated work of the Toc and Tic complexes. At the inner envelope membrane, Tic20 and Tic21 are thought to form the channel for translocation of precursor proteins into the chloroplast stroma (Kikuchi et al., 2009; Kouranov et al., 1998). Tic110, a membrane protein component of the Tic complex, has been proposed to play a dual role as receptor and channel forming protein (Balsera et al., 2009; Inaba et al., 2003). However, Tic110 topology and function are still controversial and need further confirmation (Li and Chiu, 2010). As opposed to the Toc channel, the Tic channel most certainly consists of α-helical TM segments contributed by two or possibly three different proteins. At the stromal side of the inner envelope, two heat shock proteins, Hsp93 and Hsp70, have been proposed to serve as the motor for protein translocation into chloroplasts (Nielsen et al., 1997; Shi and Theg, 2010; Su and Li, 2008). After crossing the inner envelope, the transit peptide is cleaved off by the stromal processing peptidase (SPP) (Richter and Lamppa, 1998). Once in the stroma, precursor proteins can fold if targeted to this compartment or they can be further directed to the thylakoid membrane by distinct translocation pathways.

Thylakoid Protein Import Pathways

Precursor proteins targeted to the thylakoids can be nuclear or chloroplast encoded and they can be inserted into the membrane or translocated into the lumen by one of four bacterially conserved translocation pathways: cpSec, cpTat, Alb3 and the spontaneous pathway (Jarvis and Robinson, 2004; Keegstra and Cline, 1999). Signal peptides exposed after SPP processing interact with soluble or membrane-bound receptors that direct them to the thylakoid translocation machineries. Considering our limited mechanistic understanding of Alb3 and cpSec systems, we will only review cpTat of the thylakoid translocation machineries.

Twin Arginine Translocation System in Thylakoid Membranes

The twin arginine translocation system, called Tat, transports folded proteins across the thylakoid membrane in chloroplasts and the cytoplasmic membrane in prokaryotes. Tat systems employ the proton motive force as the sole source of energy for protein transport (Berks et al., 2003; Cline and McCaffery, 2007; Lee et al., 2006; Müller and Klösgen, 2005). These unusual features differentiate Tat from other protein translocation systems that transport unfolded proteins and are energized by NTP hydrolysis.

Three membrane proteins are the components of Tat systems: cpTatC, Hcf106 and Tha4 in thylakoids or their bacterial orthologs TatC, TatB and TatA, respectively. These components are organized in homo and hetero oligomers that have been proposed to play crucial roles in the mechanism of protein transport. cpTatC and Hcf106 form a receptor complex that directly recognizes precursors carrying Tat signal peptides. The receptor complex has been characterized in detergent extracts as a multimeric complex of 500 to 700 kDa that contains only cpTatC-Hcf106 (TatB-TatC) in

a 1:1 molar ratio, suggesting ~7-8 copies of each component per complex (Bolhuis et al., 2001). Site directed crosslinking studies identify TatC as the primary receptor for the twin arginine signal peptide (Alami et al., 2003; Gérard and Cline, 2006), suggesting that each receptor complex could potentially bind 7-8 precursor proteins, although this notion has been a matter of recent debate and still remains unanswered. Support for the multivalent receptor model comes from a study of the thylakoid Tat system that showed that precursor proteins containing double cysteines in the mature domain form dimers and tetramers upon binding to single receptor complexes and are transported as oligomers (Ma and Cline, 2010). On the other hand, a structural study of *E. coli* precursor protein-bound receptor complexes suggested a maximum of two binding sites per complex (Tarry et al., 2009). However, the two bound precursors invariably were positioned next to each other forming a ~50° angle with respect to the center of the TatBC complex. Considering this, a potential of ~7 binding sites can be inferred in the *E coli* receptor complex.

Tha4 (TatA) forms a separate homo-oligomeric complex that varies in size according to the stage of protein transport (Dabney-Smith and Cline, 2009; Dabney-Smith et al., 2006; Leake et al., 2008). Binding of the precursor protein in the presence of the proton motive force triggers Tha4 assembly with the receptor complex to form the translocase (Mori and Cline, 2002). Tha4 is thought to facilitate some kind of passageway across the lipid bilayer possibly through a transient or gated channel. The proton gradient is needed for Tha4 assembly and presumably for the translocation step, since a proton counterflow is tightly coupled to protein transport (Alder and Theg, 2003a). Tat substrates vary in size from ~2 kDa to over 100 kDa, meaning that the Tat

channel has the ability to adjust its internal diameter according to the passenger protein (Berks et al., 2000). The current knowledge about the role of Tha4 (TatA) oligomers is ambiguous. TatA was initially thought to exist as a collection of homo-oligomers of different sizes (Gohlke et al., 2005). One school of thought suggested that such oligomers were selectively recruited to fit the size of the folded substrate (Sargent et al., 2006). However, *in vivo* and biochemical experiments dispute this earlier hypothesis. Real-time imaging of TatA-YFP in cells lacking a TatBC receptor showed a diffuse population of tetrameric TatA, whereas in cells containing a functional TatBC and Tat substrates, large TatA aggregates were seen that vary in size with a median of ~ 25 TatA protomers (Leake et al., 2008). Similarly, Cys-Cys crosslinking studies with thylakoid membranes show evidence of Tha4 tetramers with transmembrane domain contacts until stimulated to transport proteins, whence Tha4 oligomerizes through the carboxyl tails and forms oligomers containing at least 18 protomers (Dabney-Smith and Cline, 2009). The transient nature of Tha4 higher-oligomers has prevented a further characterization and study of its role in protein transport. Until now it has only been hypothesized that Tha4 oligomers vary in size to transport precursors of different diameters, however, the functional size of the Tha4 oligomer remains elusive. Similarly, Tha4 assembly with the receptor complex is still poorly understood.

Peroxisome Protein Import Systems

Proteins targeted to the peroxisome can be localized by two distinct pathways: the ER pathway and the peroxisome importomer pathway (Ma et al., 2011). Most peroxisomal membrane proteins are first integrated into the ER membrane by the Sec61 translocase and directed to existing peroxisomes by vesicle trafficking (Platta and Erdmann, 2007). ER derived vesicles not only contribute to peroxisome

maintenance but they can also *de novo* generate mature peroxisomes as indicated by real-time *in vivo* fluorescent microscopy studies in cells initially devoid of peroxisomes (Hoepfner et al., 2005). Targeting of peroxisome matrix proteins involves the coordinated action of multiple soluble and membrane integral complexes that collectively form the peroxisome importomer. Similarly to the Tat transport system, the peroxisome importomer machinery is capable of translocating folded and even oligomeric complexes into the peroxisome matrix without compromising the permeability barrier (Ma et al., 2011). Cytosolic cargo proteins containing peroxisome targeting signals, PTS1 or PTS2, are recognized by soluble receptors, Pex5 and Pex7 respectively (Purdue et al., 1998; Stanley and Wilmanns, 2006). Cargo-receptor complexes are then directed to the peroxisome membrane where they are recognized by the docking complex. The docking complex is composed primarily of Pex13 and Pex14 (Platta and Erdmann, 2007). Following docking, the assembled importomer translocates the cargo by an still unknown mechanism (Ma et al., 2011).The absence of an electro-chemical potential across the peroxisome membrane and the fact that no NTPs are required during the translocation step, has led to the hypothesis that protein-protein interactions could provide the energy necessary for protein translocation (Azevedo and Schliebs, 2006; Oliveira et al., 2003). After cargo release into the matrix, receptor proteins are recycled back in the cytosol by the recycling complex in a process that involves ATP hydrolysis and ubiquitination of receptor proteins (Platta et al., 2005).

Homo-oligomers of two Pex proteins, Pex5 and Pex14, have been proposed to be the structural components of the importomer channel and to participate in cargo translocation. Pex14, a major component of the docking complex, was first suggested to

form homo-oligomers in a yeast two hybrid screen (Brocard et al., 1997). This was later confirmed for endogenous and recombinant Pex14 that were shown to form homo-oligomers of different sizes, from dimers to octamers, by chemical cross-linking and sedimentation assays (Itoh and Fujiki, 2006). In this study, a conserved coiled-coil domain in Pex14 was shown to be required for oligomerization. The topology of Pex14 is still controversial. Membrane extraction and protease protection assays in most organisms suggest that Pex14 is an integral membrane protein, however, in *S. cerevisiae* Pex14 can be extracted from the membrane at a pH 11.5 (Azevedo and Schliebs, 2006). Although Pex14 topology is still controversial, its predicted 16-residues TM domain and its ability to oligomerize make it a good candidate for being a structural element of the cargo conducting channel (Azevedo and Schliebs, 2006). The oligomeric state of the receptor Pex5 in its cytosolic form has been a matter of recent debate with some studies supporting a monomeric form and others a tetrameric form. Support for monomeric Pex5 comes from structural studies using in solution small angle x-ray scattering (Shiozawa et al., 2009). On the other hand, evidence for tetrameric Pex5 comes from *in vivo* studies using the split-ubiquitin technique that reported Pex5:Pex5 interactions in yeast (Eckert and Johnsson, 2003) and from *in vitro* assays with recombinant Pex5 appearing as tetramers by sizing chromatography (Schliebs et al., 1999). Recently, structural and functional roles for Pex5 and Pex14 homo-oligomeric assemblies were suggested after the reconstitution of a minimal peroxisome importomer (Meinecke et al., 2010). In this study, affinity purified yeast complexes contained Pex5 and Pex14 in a 1:1 ratio and when reconstituted into planar lipid bilayers displayed a channel activity induced by cargo-receptor interactions. Interestingly, the observed

conductances varied with the size of the cargo-receptor complex used in the assay showing a maximum pore size of 9 nm for a cargo-receptor complex of 750 kDa. Considering the apparent size of the pore-forming complex, 600-800 kDa, it was proposed that Pex5 and Pex14 must form some kind of homo and/or hetero-oligomeric assembly at the open pore (Meinecke et al., 2010). The docking domain of Pex5 in the cargo-receptor complex is mainly unstructured in solution (Carvalho et al., 2006) but has the potential to form up to 5 amphipathic helices upon docking that could display pore forming properties and contribute in the formation of the transient pore (Meinecke et al., 2010).

Conclusions

Protein oligomerization is a common phenomena in cellular systems. In fact, a survey of the Protein Data Bank in 1993 indicated that ~35% of the proteins in a cell are oligomeric (Jones and Thoronton, 1996), and of those, most are homo-oligomers (Goodsell and Olson, 2000). Oligomers can be classified according to their composition (homo or hetero-oligomers), their duration and strength (stable or transient), their ability to respond to stimuli (pH, nucleotide binding, membrane binding, phosphorylation, etc) and their mode of interaction (indefinite or discrete) among others (Ali and Imperiali, 2005). These features enable oligomeric complexes to play essential roles in processes such as cell division (microtubules), vesicle trafficking (actin filaments), membrane fission (dynamins), and energy transduction (ring motors), that monomeric proteins would not be able to perform.

Homo-oligomers of membrane proteins are best characterized in complexes of the bacterial outer membrane. The functions of some of these multimeric complexes include catalytic cooperativity (OmpLA), active sites multivalency (trimeric autotransporters),

and structural scaffolding (TolC) (Meng et al., 2009). Homo-oligomeric complexes involved in protein translocation systems show specific functions that include: increased stability (Sec channels), coordinated transport activity (Tim22), and transient pore formation (Tat and peroxisome importomer). A detailed characterization of the role of homo-oligomeric assemblies in Tat systems is fundamental for understanding the mechanism of protein translocation. Of special interest is the functional size and dynamics of Tha4 (TatA) oligomers, the component thought to facilitate protein movement across the membrane.

CHAPTER 2
METHOD DEVELOPMENT FOR MEMBRANE PROTEIN QUANTIFICATION

Summary

Low abundance membrane proteins are difficult to quantify with any accuracy. Absolute mass spectrometry and immunoblotting are typical methods of choice. We found that immunoblotting using soluble antigens as standards was very inaccurate due to differential behavior of antigen and membrane protein with respect to electroblotting and antibody reactivity with blots. A novel method was developed that employs radiolabeled *in vitro* translated full-length membrane proteins as standards that are quantified by radiolabel counting. Proof-of-concept experiments with three different membrane proteins indicated an error of 5 to 8%, a dramatic improvement over previous methods. Our method is generally applicable, requiring only a good antibody, relevant cDNA, and a commercial or homemade *in vitro* translation system. Moreover, it is simple, inexpensive, and can be used for routine analysis.

Introduction

Membrane proteins represent ~26% of the proteome in eukaryotes (Fagerberg et al., 2010). They play many essential roles in signaling, transport, and biogenesis in different organelles and subcellular domains. Recent advances in methods such as fluorescent microscopy, mass spectrometry, and specific attachment of probes and tags, have greatly improved our understanding of their functions (Gingras et al., 2007; Joo et al., 2010). However, knowledge of membrane protein function and mechanism still trails behind their soluble counterparts. This is mainly explained by the difficulties in obtaining structural information, in expression and purification protocols, and in developing *in-vitro* reconstituted assays, among others. A fundamental step towards

understanding membrane protein function is to develop quantitative methods to accurately measure the concentration of membrane proteins, especially low abundance membrane proteins. Such a method would enable studies of their stoichiometry in the membrane and in solubilized complexes. Only a few methods have been developed to quantify membrane proteins. These include absolute mass spectrometry quantification and quantitative immunoblotting (Barnidge et al., 2003; Gerber et al., 2003). Absolute mass spectrometry quantification requires access to a LC MS/MS mass spectrometer with multiple reaction monitoring capabilities (MRM) and a considerable investment in time and money simply to prepare for the measurement. On the other hand, quantitative immunoblotting can give accurate measurements of membrane protein, but requires appropriate standard proteins.

We have investigated methods for quantifying the membrane protein components of the Twin arginine translocation system (Tat) present in the thylakoids of chloroplasts and the cytoplasmic membrane of prokaryotes. Thylakoid translocases are low abundance membrane proteins that play a critical role in the targeting and localization of lumenal and membrane integrated proteins (Cline and Theg, 2007; Henry et al., 2007). Their components are typically present in tens of thousands per thylakoid, compared to the proteins of the photosynthetic complexes, which are present at ~ 1 million copies per thylakoid. To date, study of translocase components has primarily been limited to qualitative methods with a few examples of semi-quantitative studies (Jack et al., 2001; Jakob et al., 2009; Mori et al., 2001). The Tat system consists of three membrane proteins, called cpTatC, Hcf106 and Tha4 in thylakoids and TatC, TatB and TatA in bacteria. Precursor proteins transported by Tat are first recognized by the receptor

complex, a ~700 kDa complex formed only by cpTatC and Hcf106. In the presence of a proton gradient, a Tha4 oligomer is recruited to the precursor-bound receptor complex and the precursor is transported by a still unknown mechanism. Different models propose that Tha4 would serve as the precursor passageway across the membrane (Bruser and Sanders, 2003; Sargent et al., 2006). Previous quantifications of Tat components in pea chloroplasts and *E. coli* by different semi-quantitative methods have produced components stoichiometry that support this model (Jack et al., 2001; Mori et al., 2001). However, a recent study of *Arabidopsis* thylakoids, using similar methods, found a very different stoichiometry that questioned the proposed role for Tha4 (TatA) as the protein-conducting channel (Jakob et al., 2009). In addition to the debate on Tha4's role in protein transport, the lack of quantitative information regarding the number of binding sites in the receptor complex and the functional size of the Tha4 oligomer, limits our understanding of the mechanism of Tat transport.

Here, we modified the traditional semi-quantitative immunoblotting protocol to have an accurate and reliable way of quantifying Tat components and precursor proteins. The method is relatively simple and generally applicable to membrane and soluble proteins alike, provided that antibodies to the proteins are available. The method uses radiolabeled *in vitro* translated full length Tat components as standards of known concentration. The concentration of standards is determined after isotope dilution experiments to estimate the specific radioactivity of the tracer amino acid present in the wheat germ (WG) extract used for *in vitro* translation. Protein concentrations in test samples are estimated by immunoblotting and densitometry analysis within the linear range of standards. The accuracy of the method was dramatically improved by using

full-length proteins as standards and a careful accounting of the gel extraction efficiencies for each component. A proof-of-concept experiment demonstrate that the method permits quantitative studies of low abundance membrane proteins in complex native environments. In addition, the obtained quantities of Tat components support the role of Tha4 (TatA) as the protein-conducting component of the Tat system.

Results

Previous semi-quantitative methods to quantify Tat components in thylakoids used immunoblotting of the endogenous components compared to antigen standards that consisted of a bacterially expressed soluble domain of the component in question. The assumption was that the standards would behave similarly as the endogenous components. We tested this by using radiolabeled soluble domain cpTatC (sdTatC) and the full-length cpTatC proteins obtained by *in vitro* translation with a wheat germ system. Radiolabeled proteins were solubilized in SDS buffer and analyzed by SDS-PAGE in duplicate, one gel for fluorography and another gel for immunoblotting as described in figure legend (Fig. 2-1). The two translation products were then quantified by two methods, by radiolabel counting and by the immunoblot signal compared to the bacterially expressed cpTatC soluble domain (Fig. 2-1, A and B). If the assumption was true, the molar ratio between soluble domain proteins and full-length proteins should be the same before and after immunoblotting. Surprisingly, we found that soluble domain alone behaves very differently during electro-transfer to blotting membranes and/or reaction with antibody than the full-length cpTatC protein (Fig. 2-1D). This experiment indicated that using the soluble domain as standard in immunoblotting overestimated the amount of full-length cpTatC and moderately underestimated the *in vitro* translated soluble domain. This differential behavior is probably due to the different molecular

masses of cpTatC ~ 33kDa vs. sdTatC ~ 10 kDa, and especially the different hydrophobicities, e.g. the GRAVY index for cpTatC 0.46 and sdTatC -0.99. The different behavior of stromal domain proteins versus full-length proteins was not reduced by using polyvinylidine fluoride versus nitrocellulose membranes or different gel systems (Laemmli versus tricine SDS-PAGE). A similar experiment with Hcf106 also found that sdHcf106 standards overestimated full-length Hcf106 (data not shown). We sought to eliminate this systematic error in the quantification of Tat components by using full-length proteins as standards of known concentration. However, due to the multiple difficulties in expressing and purifying thylakoid Tat components, we used WG *in vitro* translated (IVT) full-length proteins as standards of known concentration.

Determining the Concentration of Standards

The concentration of radiolabeled *in vitro* translated standards can be determined by scintillation counting of bands extracted from SDS gels if the specific radioactivity of translation products is known. The specific radioactivity of translation products depends on the amount of unlabeled leucine (or other amino acid depending on the isotopically labeled amino acid) present in the wheat germ extract and the amount of tritiated leucine added to the translation mixture. Isotope dilution experiments were used to determine the concentration of unlabeled leucine in each the wheat germ extract preparation (Patrick et al., 1989). For each calibration, three different mRNAs were translated with the same amount of radiolabel and different amounts of unlabeled leucine. The reciprocal of the radioactivity extracted from each band was plotted against the total leucine concentration in the reaction (Fig. 2-2, B and C). The amount of unlabeled leucine contributed by the WG is indicated by the intercept with the y-axis. The concentration of unlabeled leucine obtained with the three different mRNAs was 3.8

μM (SD 0.22). Leucine was not a limiting factor in the reaction because immunoblots of translation reactions gave essentially the same signal for the range of leucine concentrations in the experiment (Fig. 2-2 A, lower panel). In a standard translation reaction the amount of WG extract is 60% vol/vol and the amount of ^{3}H leucine added is 45 μCi (~0.3 nmol ^{3}H-leu). Considering the amount of unlabeled leucine present in the WG extract, our translation products have a specific radioactivity of ~ 51 μCi/ nmol leu.

Extraction Efficiencies of *In Vitro* Translated Proteins

Radiolabeled IVT proteins were routinely quantified by extracting gel slices with TS-2 (RPI) followed by scintillation counting (Appendix Experimental Procedures). Thus, it's not only important to have a well-calibrated scintillation counter, but also to determine the efficiency of extracting different proteins from polyacrylamide gels. Our liquid scintillation system was checked for tritium counting efficiencies and a new quench correction curve was generated with a set of new tritium quenched standards (Perking Elmer). Color quench correction was also checked with samples containing a known amount of isotope and increasing amounts of chlorophyll. Extraction efficiency was determined with two different approaches. His-tagged proteins were purified by metal affinity chromatography and the radioactivity determined by direct counting was compared to that obtained by extracting proteins from gels (Fig. 2-3 A). Second, proteins were first integrated into thylakoid membranes by chloroplast import, thylakoid integration, or binding of precursor proteins and similarly analyzed (Fig. 2-3 B). Gel slices were obtained for the main band of the purified protein, and also for the rest of the lane, above and below the main band (Fig. 2-3 C). Table 2-1 summarizes the results obtained for extraction efficiencies.

As indicated in Table 2-1, the main band representation of the total radioactivity varied from 60% to 89% depending on the protein in question. Both approaches, Ni^{++} purification and membrane association, yielded very similar results with only small differences in their values for main band representation. cpTatC, the most hydrophobic of all, showed some aggregation that can be seen in extended exposure of fluorograms and immunoblots of IVT cpTatC (Fig. 2-3 B). Aggregates of translation products accounted for the radioactivity extracted above the main band since no radioactivity could be detected in a mock translation. Interestingly, this aggregation is reduced in the membrane associated protein, indicating that cpTatC is less prone to aggregation when inserted in a lipid bilayer. Total radioactivity extracted and main band representation were used as correction factors in our novel quantitative immunoblotting method. Total radioactivity extracted with Nickel purified proteins was used as extraction efficiency to correct the amount of IVT standards. The values obtained for the main protein band and above main band in membrane associated proteins were used as correction factors in our immunoblotting quantification of total endogenous components in thylakoid membranes.

Proof of Concept Experiment

In order to crosscheck our novel quantification procedure we determined the levels of cpTatC, Hcf106, and Tha4 in thylakoid membranes after integrating additional Tat components by import/integration of radiolabeled translation products. In this proof of concept experiment, the additional components that derive from *in vitro* translation are determined by immunoblotting (i.e. the increase in immunoblot signal over mock-import/integrated thylakoids) and compared to the amounts determined by radiolabel counting. The results are shown in Fig. 2-4. The error of our quantitative immunoblot

method to estimate the amount of imported/integrated TatC, Hcf106 and Tha4 was 8, 5 and 5%, respectively, a dramatic improvement over previous methods. Thus, this approach can be used to determine not only the concentration of Tat components in thylakoids, but also of *in vitro* translated precursor proteins.

Re-evaluation of the Quantities of cpTat Components in Pea Chloroplasts

The role of Tha4 (TatA) was questioned by a recent study in *Arabidopsis* (Jakob et al., 2009) that found a different stoichiometry of Tat components than that reported for pea thylakoids and *E coli* Tat components. They found that TatA was the least abundant of the three components, challenging its proposed role as the protein conducting channel. For this reason we decided to use our improved quantification method to re-evaluate the stoichiometry of Tat components in pea chloroplasts. To do this, we prepared intact chloroplasts from three biological replicates and used them to isolate thylakoid membranes. Intact chloroplasts and washed thylakoids were used for quantification to prevent an underestimation of Tha4 and Hcf106, which can be found in small amounts in envelope membranes after fractionation (Fincher et al., 2003). Chloroplasts and thylakoids were analyzed by SDS-PAGE and immunoblotted for quantification with IVT full-length protein standards. Table 2-2 shows the number of molecules per chloroplast, per thylakoid and the ratio of components.

The concentrations and stoichiometry of cpTat components reported previously were 1:5:8 (cpTatC:Hcf106:Tha4) (Mori et al., 2001). Using full-length *in vitro* translated standards we found that cpTatC and Hcf106 maintain a similar ratio of 1:5 but with different concentrations in the membranes (Table 2-2). As expected, the amounts of cpTatC and Hcf106 did not significantly vary between intact chloroplasts and thylakoids. The concentration of Tha4 in thylakoids is similar to the one reported previously but with

a higher ratio to cpTatC i.e. 1:15. In intact chloroplasts, the ratio of Tha4 to cpTatC was higher than in thylakoids and closer to the stoichiometry in *E coli*, i.e. 1:24.

Conclusions

Taken together, these results demonstrate that when using appropriate standards, immunoblotting provides an accurate and reliable method for quantifying low-abundance membrane proteins. This protocol offers a tool to study the relative and absolute abundance of membrane proteins when inserted in a lipid bilayer or after solubilization and purification under native conditions. When studying membrane protein receptors, this method can be used to determine the number of binding sites per receptor and identify cooperativity between binding sites. Reorganization or rearrangements in membrane protein complexes can also be studied upon placing appropriate affinity tags in one of the complex components. An important advantage of this immunoblotting method over others is that it is inexpensive and doesn't require special instruments, making it ideal as a routine analysis to measure the concentration of membrane proteins.

Table 2-1. Extraction efficiencies of radiolabeled proteins from dried gels

	In solution	Gel extracted							
		Main band		Above main band		Below main band		Total radioactivity extracted	
Protein	Ni^{++} purified or membrane associated (%)	Ni^{++} purified (%)	Membrane associated (%)	Ni^{++} purified (%)	Membrane associated (%)	Ni^{++} purified (%)	Membrane associated (%)	Ni^{++} purified (%)	Membrane associated (%)
cpTatC	100	60 (0.6)	67 (1.3)	19 (0.5)	11 (0.2)	14 (0.8)	8 (0.2)	94 (0.7)	86 (2.9)
Hcf106	100	72 (0.4)	73 (0.1)	3 (0.2)	3 (0.03)	15 (0.3)	9 (0.01)	90 (0.7)	85 (0.1)
Tha4	100	71 (1.0)	79 (1.5)	9 (0.7)	7 (0.3)	5 (0.2)	5 (0.1)	85 (1.6)	91 (1.2)
tOE17	100	89 (0.5)	82 (0.6)	1 (0.1)	3 (0.3)	5 (0.04)	5 (0.1)	95 (0.6)	90 (0.7)

Reported numbers are averages of three technical replicates. Standard deviation is indicated in parenthesis.

Table 2-2. Re-evaluation of Tat components in pea chloroplasts and thylakoids

	Intact chloroplasts (molec/cp)		Thylakoids (molec/Thy)			
Protein	Average	SD	Average	SD	Stoichiometry chloroplasts	Stoichiometry thylakoids
cpTatC	8,200	(400)	9,100	(150)	1	1
Hcf106	39,600	(2,300)	38,300	(1,700)	~5	~4
Tha4	196,000	(13,600)	134,600	(33,300)	~24	~15

Reported numbers are average of three biological replicates. Standard deviation is indicated in parenthesis.

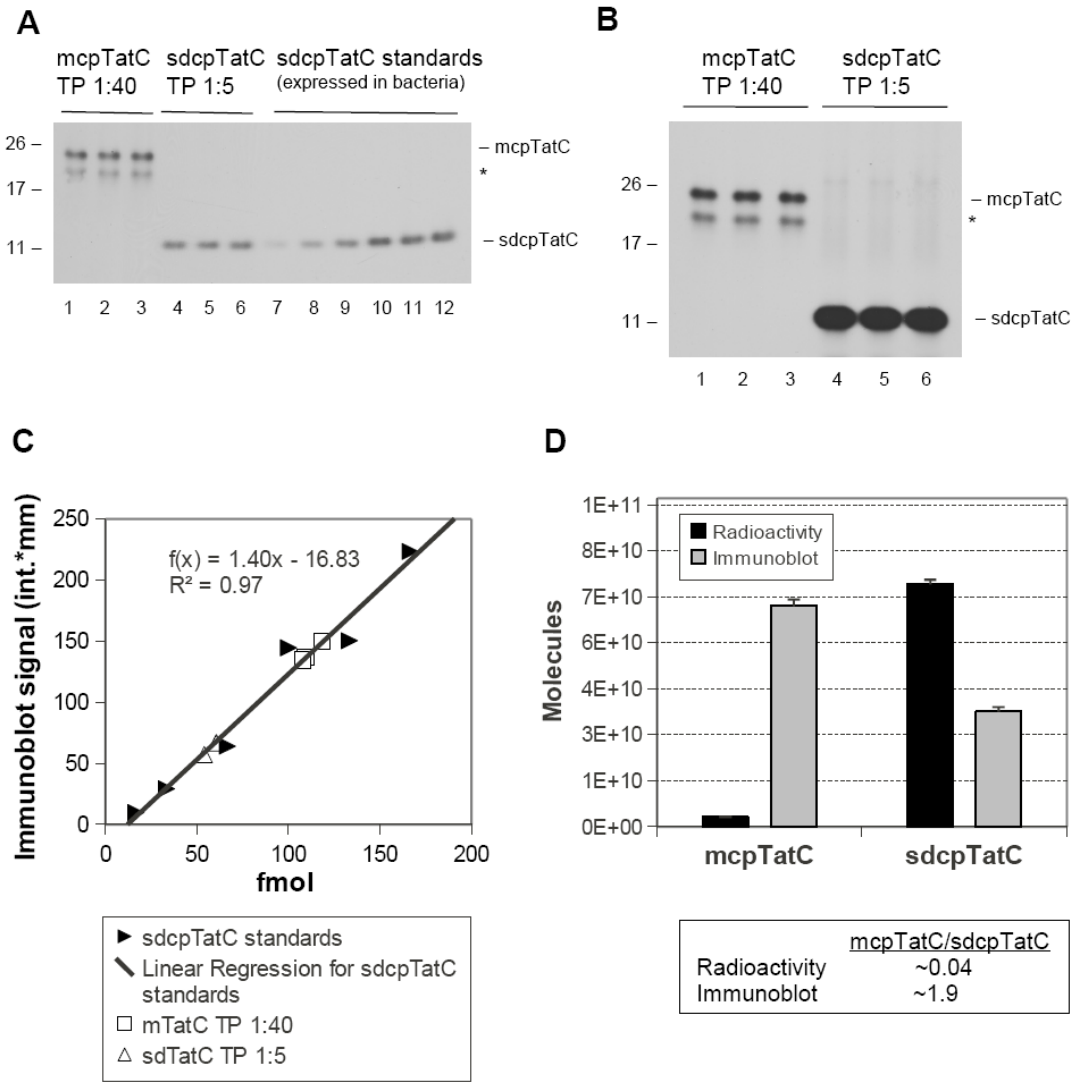

Figure 2-1. Differential behavior between soluble-stromal-domains and full-length proteins in immunoblotting. Full-length cpTatC (mcpTatC) and stromal-domain cpTatC (sdcpTatC) were *in vitro* translated and diluted in order to have similar immunoblot signal intensities. Antibodies against sdcpTatC (Mori et al., 2001) were used for immunoblotting. Samples were loaded in triplicate and analyzed in a 10% tricine SDS-PAGE followed by immunoblotting (a) or fluorography (b). Electroblotting and detection were performed as described in Appendix Experimental Procedures. Immunoblot quantification by densitometry analysis was done within the linear range sdTatC standards of known concentration expressed in bacteria (c). Proteins were quantified by scintillation counting as described in Appendix Experimental Procedures. Comparison of the amounts of protein quantified by scintillation counting versus immunoblotting (d). (*) degradation product of mTatC not considered in quantifications.

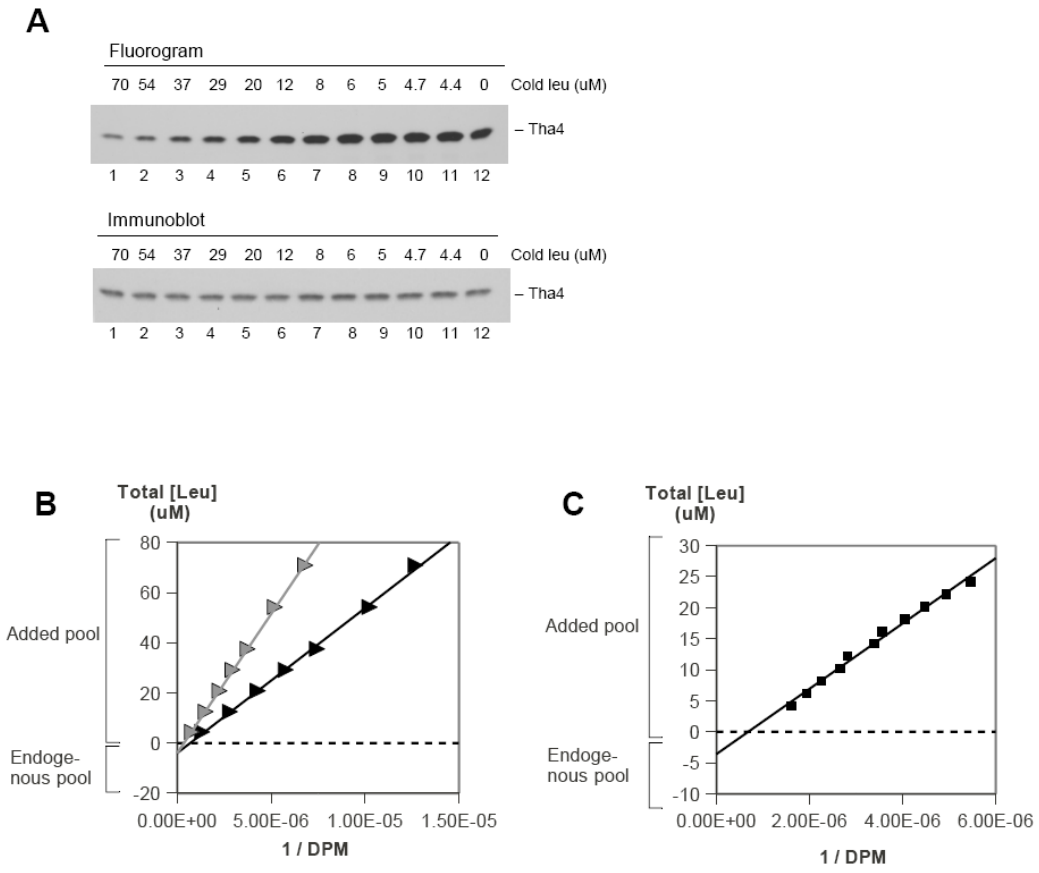

Figure 2-2. Isotope dilution analysis to determine translation product's specific radioactivity. WG translation reactions with increasing amounts of unlabeled leucine were incubated at 25°C for 1 h and analyzed by SDS-PAGE followed by fluorography and immunoblotting (A, upper and lower panels respectively). Bands with radiolabeled translation products were excised from gels and prepared for scintillation counting as described in Appendix Experimental Procedures. Isotope dilution analysis establishes that when plotting the concentration of total leucine added to the reaction (added unlabeled leu plus added ^{3}H-leu) versus the reciprocal of the radioactivity, the size of the endogenous pool of unlabeled amino acid corresponds to the negative intercept of the regression line with the y-axis (y = total [leu] = [unlabeled leu]+[^{3}H-leu] = m*1/dpm + c, where m is the slope of the regression line and c the intercept with the y-axis). Three different mRNAs (mTatC, Tha4 and tOE17) were used for isotope dilution experiments and plotted (B and C).

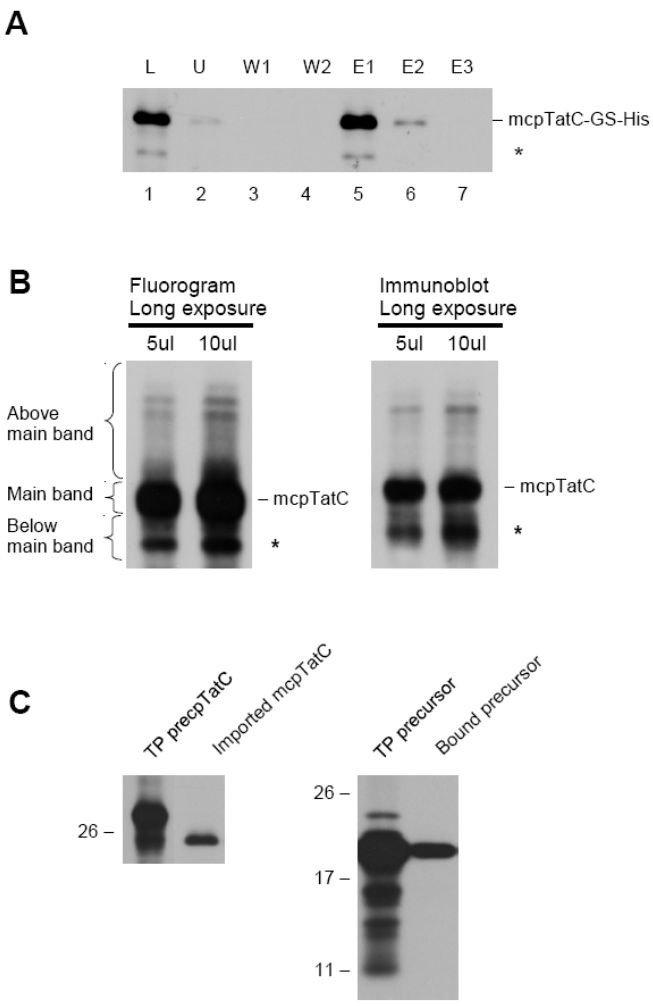

Figure 2-3. Gel extraction efficiencies of *in vitro* translated proteins. *In vitro* translated His tagged Tat components and precursor protein were purified by Ni-affinity chromatography following the manufacturer instructions (A) mTatC-GS-His purification is shown as a representative example. Gel slices were obtained for the main band and for above and below the main band of purified proteins (B). Proteins were extracted using TS2 and incubation at 50°C for 6 hours as described (Cline, 1986). Gel extracted proteins were compared to in-solution proteins after scintillation counting to obtain the extraction efficiency. (*) degradation product mTatC. Purified proteins were also obtained after import, binding or integration reactions with thylakoid membranes (B). IVT mTatC analyzed by fluorography and immunoblotting (C).

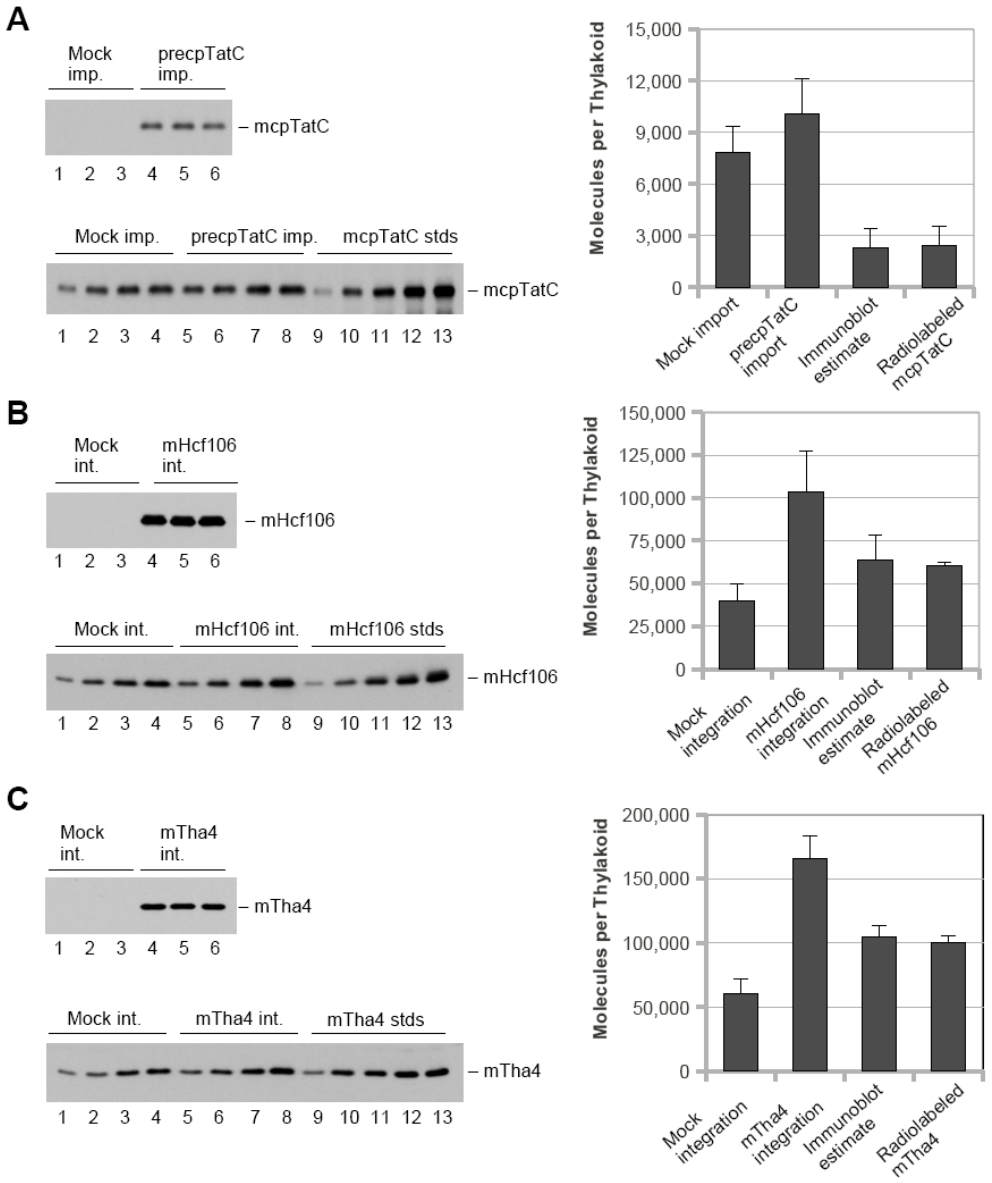

Figure 2-4. Proof-of-concept experiment for Tat components quantification. preTatC and mock import reactions were each performed in 3 replicates for 1 hour as described in Appendix Experimental Procedures. Chloroplasts were repurified after import and treated with thermolysin for 40 min on ice previous to thylakoid isolation. Isolated thylakoids were analyzed by SDS-PAGE followed by fluorography (A, upper panel). Hcf106 and Tha4 integration were performed by incubating TP with thylakoid membranes at 25°C for 20 min as described in Appendix Experimental Procedures. Membranes were recovered by centrifugation, washed twice and resuspended in IBM buffer before being analyzed by SDS-PAGE and fluorography (B and C, upper panels). Imported/integrated components were quantified by scintillation counting as described in Appendix Experimental Procedures. Endogenous components plus imported/integrated components were quantified by immunoblotting with

IVT standards of known concentration of the component in question (A, B and C, lower panels). For immunoblotting quantification, each replicate was analyzed in a separate gel where a dilution series of mock treated membranes and import/integrated membranes were compared to the linear range of IVT full-length standard proteins (only one replicate is shown).

CHAPTER 3
STOICHIOMETRY FOR BINDING AND TRANSPORT IN THE TWIN ARGININE TRANSLOCATION SYSTEM

Summary

Twin arginine translocation (Tat) systems are characterized for transporting folded proteins across membranes. Precursor protein transport is a four steps cyclical process where the translocase only assembles transiently. In the binding step, precursor proteins are recognized by the multimeric receptor complex. The number of binding sites in the receptor complex has been recently a matter of debate and remains to be determined in the thylakoid Tat system. Upon energizing the membranes with a proton gradient, Tha4 is recruited to the precursor-bound receptor complex and forms homo-oligomers that are thought to facilitate precursor translocation across the membrane. Here, we used saturation binding analysis of the OE17 precursor and transport kinetics to determine the stoichiometry of Tat components for binding and transport.

Introduction

The Tat system is composed of stable and transient higher-order oligomeric assemblies. Hcf106 and cpTatC form a 700 kDa receptor complex that is thought to be a stable structure containing 7-8 copies of each component(Bolhuis et al., 2001). The role of such a large complex and the number of binding sites for precursor proteins are still unknown. Tha4 is a single transmembrane (TM) domain protein with a predicted amphipathic helix and a soluble C-tail that oligomerizes according to transport conditions (Dabney-Smith and Cline, 2009; Dabney-Smith et al., 2006; Leake et al., 2008). In de-energized membranes or in the absence of bound precursor proteins Tha4 exist as tetramers. Upon precursor binding in the presence of a proton motive force, Tha4 forms higher-order oligomers that are thought to provide a passageway for

precursor proteins across the membrane (Berks et al., 2003; Bruser and Sanders, 2003; Cline and Theg, 2007). The functional size of Tha4 homo-oligomers, a key aspect of Tat transport, still remains unknown.

In the present studies, we have used quantitative biochemical analyses to determine the valency of the large Hcf106-cpTatC complex for binding and transporting precursor proteins. Our results indicate that each cpTatC subunit can bind a precursor protein, suggesting that each complex, when saturated, contains 7-8 precursor proteins. We find no evidence of cooperativity between binding sites from analysis of binding saturation experiments, suggesting that each site binds a precursor protein independently of any other site. Comparison of transport rates from ~20% occupied complexes vs. saturated complexes leads us to postulate that, when Tha4 is in excess, all sites can transport their bound precursor proteins independently and simultaneously. Analysis of transport kinetics from the bound state of membranes with different amounts of Tha4 per bound precursor protein indicate that for the OE17 precursor protein, a Tha4 oligomer of ~28 protomers is the minimal functional Tha4 for optimal transport rates. The implications of our findings for the mechanistic strategy of Tat systems are discussed.

Results

In vitro translated tOE17 V-20F was used as precursor protein for this study. This is a slightly modified version of the OE17 precursor that lacks several non-essential amino proximal residues and places a phenylalanine at the twin arginine (RR) +2 position, resulting in higher affinity binding (Gérard and Cline, 2007; Ma and Cline, 2000). The RR +2 F is found in most bacterial Tat substrates, where it plays an important role in transport efficiency (Stanley et al., 2000). *In vitro* translated precursor

protein was used because of its very low level of non-specific binding, i.e. compared to bacterially expressed precursor proteins (Ma and Cline, 2000).

Also employed here is a method to accurately quantify both precursor protein and endogenous Tat components. In this method the precursor protein is quantified by radiolabel counting with appropriate corrections for the actual specific radioactivity of isotope in the translation reaction and the recovery of proteins extracted from gel slices. Tat components are quantified by immunoblotting using radiolabeled full-length proteins as standards. The advantage of this approach is that standard proteins used in immunoblotting are chemically identical to test proteins and quantification of precursor proteins as well as Tat components is ultimately dependent on radiolabel counting. This approach to quantifying precursor protein and Tat components has an error of ~5-8%, thereby enabling the studies reported here.

Precursor Proteins Bind to the Tat Receptor with High Affinity and a Very Low Rate of Dissociation

In developing an assay for precursor protein binding to thylakoid membranes, it was necessary to assess rates of association and dissociation of the precursor protein. In preliminary experiments, we found that binding occurred faster than we could practically determine with our assay, i.e. less than 5 min (data not shown). Because our binding reactions are carried out for 60 min, equilibrium is assured even with low concentrations of precursor protein. The dissociation rate of membrane-bound precursor protein was tested in several ways. When thylakoids recovered from saturation binding assays were incubated with buffer, less than 3% of bound precursor protein was released to the supernatant in 50 min of incubation at 25°C (data not shown). A more rigorous test of dissociation involved incubating thylakoids saturated

with radiolabeled precursor protein (see below and Fig. 3-1) with a saturating concentration of unlabeled precursor protein. Under these conditions, any radiolabeled precursor protein that dissociated from its binding site would be replaced by unlabeled precursor protein and the rate of dissociation could be estimated by appearance of radiolabeled precursor protein in the supernatant. As can be seen in Fig. 3-1, the amount of displaced radiolabeled precursor protein after 60 min at 0°C was low; 85% of radiolabeled precursor protein remained membrane bound (Fig. 3-1 A, B and C). Only when the incubation temperature was increased to 25°C was a substantial percentage of radiolabeled precursor protein released to the supernatant (Fig. 3-1 A, B and C). Curiously, some of the precursor protein released into the supernatant at 25°C was the size of mature OE17 (mOE17), suggesting it could have been processed by a protease in the wheat germ extract. Overall, these experiments indicated that the precursor protein has a very low dissociation rate from its binding site at 0°C, such that membrane recovery by centrifugation and washing would not significantly reduce the amount of bound precursor protein.

Estimation of Non-specific Binding

The specificity of binding to thylakoids was examined in several ways: binding of the non-functional twin lysine precursor protein, binding to thylakoids pretreated with antibodies to Tat receptor components, and binding to membranes pre-treated with protease. As with the experiment in Fig. 3-1, binding reactions were conducted with concentrations of precursor protein that would saturate the binding sites. As indicated in Fig. 3-2 A, pretreatment with antibodies to cpTatC, the primary receptor component (Alami et al., 2003; Gérard and Cline, 2006) reduced precursor protein binding to ~10% of that with mock treated membranes (lane 6). This reduction did not occur if the cpTatC

antigen (3.75 µM) was included in the antibody binding reaction (lane 5). Similarly, protease pretreatment of the membranes reduced binding to ~8% of control mock treated membrane (Fig. 3-2 A, lanes 7 and 8). Consistent with these values, binding of a non-functional KK precursor protein was ~7% of that of the RR precursor protein. This level of KK-precursor protein binding was unaffected by IgG pre-treatment (Fig. 3-2 B, lanes 2 to 6) or by protease-pretreatment of thylakoids (lanes 7, 8). These results indicate that under the conditions used to measure binding in this study, a low percentage of precursor proteins bind non-specifically to the lipid bilayer (Fig. 3-2 B, lanes 7 and 8). Moreover, they indicate that binding of the KK-precursor protein is a representative measure of non-specific binding.

The Stoichiometry of Precursor Protein Binding to the Tat Receptor Complex

Saturation binding experiments were performed as a first approach to determine precursor protein binding stoichiometry to cpTatC. Thylakoids recovered from each binding reaction were analyzed by SDS-PAGE/fluorography to quantify precursor protein (Fig. 3-3 A, upper panel, lanes 2 to 10) and SDS-PAGE immunoblotting in parallel to quantify cpTatC (data not shown). The expected binding saturation curve was obtained but with gradually increasing binding at upper concentrations. Non-specific binding, estimated with KK precursor protein (Fig. 3-3 C), was linear in the concentrations range used in the assay. Subtracting non-specific binding at each concentration from the RR precursor protein binding data produced a specific binding curve that asymptotically approached saturation at higher precursor protein concentrations (Fig. 3-3 C). Specifically bound precursor protein data was fit by nonlinear regression to a single-site binding model to obtain maximum binding (Bmax; Fig. 3-3 C), which was divided by the amount of cpTatC in each assay to give a binding

stoichiometry of 1.36 (SD 0.2) precursor proteins per cpTatC for four biological replicates. Essentially the same stoichiometry was obtained by Scatchard analysis of the binding data (Fig. 3-3 D) The dissociation constant (Kd) from four biological replicates was 1.2 nM (SD 0.1) (Fig. 3-3 C).

Binding curves were also analyzed for any indication of cooperativity. The Hill coefficient for the four binding curves obtained from non-linear regression of a binding model that contains a Hill coefficient was 1.1 (SD 0.2). Because in practice, cooperativity is most evident in the middle region of the binding isotherm, a binding experiment with additional data points in this region of the curve was conducted and the data subjected to Hill analysis. The Hill coefficient in this more accurate determination was 1.2 (Fig. 3-4). This indicates that there is no cooperativity of binding, i.e. no interaction between sites.

The Increase in Binding Sites that Result from Importing precpTatC into Chloroplasts is ~1 per Imported cpTatC

The precursor/cpTatC binding stoichiometry at saturation was determined by two additional approaches that minimized non-specific binding. First, *in vitro* translated radiolabeled pre-cpTatC was imported into chloroplasts, and the thylakoids isolated from those chloroplasts were used for saturation binding reactions (Fig. 3-5 A). The amount of precursor protein bound was compared to the amount bound by thylakoids isolated from a mock import reaction. We hypothesized that if each cpTatC is binding one precursor protein, we should see an increase in binding equivalent to the molar amount of TatC imported. Note that in this approach the increase in binding and imported cpTatC are determined by radiolabel counting alone, and also that non-specific binding does not affect the measurement. The ratio of precursor protein to

cpTatC by this method was 0.92:1 (SD 0.02) (Fig. 3-5 B). These results indicate that, if all imported cpTatC are functional, imported cpTatC proteins were each capable of binding one precursor protein.

Stoichiometry of Precursor Protein per cpTatC Determined with Detergent Solubilized Precursor Protein-bound Tat Receptor

A third approach involved saturating receptors, then solubilizing and purifying the complex by immuno-affinity to anti-Hcf106 IgG beads. The intention was to eliminate the contribution of the lipid bilayer to non-specific binding. The SDS eluate of washed beads was quantified for precursor protein and cpTatC. In three biological replicates ~65% of bound precursor protein was recovered in the supernatant after digitonin solubilization and 35% in the pellet (Fig. 3-6, A and C). This was somewhat surprising because immunoblot analysis of the same samples showed that almost all cpTatC was recovered in the supernatant (Fig. 3-6 B, lanes 1 and 2). Only small amount of precursor protein and undetectable levels of cpTatC were in the flow through and wash fractions of the immunoprecipitation, and the recovery of precursor protein was 85% (SD 8.1) (Fig. 3-6, A and C). Quantification of the eluate (Appendix Experimental Procedures; Fig. 3-6 D) gave a stoichiometry of precursor protein to cpTatC of 0.83:1 (SD 0.21). A similar ratio was also obtained when a His-tagged precursor protein was used in the binding reaction and the digitonin-solubilized complex was purified by metal ion affinity chromatography (see below, Fig. 3-7). In summary, the ratio of precursor protein to cpTatC obtained by the three methods: binding saturation curves, increase in binding after cpTatC import, and purification of fully occupied complexes, was 1.36, 0.92 and 0.83 respectively. The average of the 3 methods, 1.04, indicates a stoichiometry of 1 precursor protein per cpTatC at saturation. In other words, each large receptor

complex contains ~8 precursor protein binding sites. Since cpTatC is the primary binding site for the signal peptides of precursor proteins, this suggests that each cpTatC-Hcf106 pair functions as a precursor protein-binding site.

Bound Precursor Proteins are Dislodged from the Receptor Complex During BN-PAGE Analysis

Many previous experiments in our lab have analyzed precursor protein association with the Tat receptor complex by Blue Native Polyacrylamide Gel Electrophoresis (BN-PAGE). Even under saturating conditions, precursor protein binding only up-shifted the molecular Mr of the receptor complex by ~ 50 kDa rather than the ~200 kDa expected for binding 8 precursor proteins (Fincher et al., 2003). To address this issue, binding sites were saturated with a precursor protein containing a His6 tag at its carboxyl terminus. Precursor-bound complexes were solubilized with digitonin and purified by metal affinity chromatography as described in Appendix Experimental Procedures. Purification fractions were analyzed by SDS-PAGE and BN-PAGE (Fig. 3-7, A and B respectively). As expected, quantification of precursor protein and cpTatC in the Ni-NTA eluate after SDS-PAGE indicated ~0.9 precursor proteins per cpTatC. However, quantification of precursor and cpTatC in the 700 kDa band of BN-PAGE gave a ratio of precursor protein to cpTatC of ~0.2. The significant amount of radiolabel smeared below the 700 kDa band that migrated at 23 kDa suggests that precursor proteins were dislodged from the receptor complex during BN-PAGE electrophoresis (Fig. 3-7 C).

All Binding Sites are Independently Functional for Transport

Transport of receptor-bound precursor proteins is a single turnover reaction. It occurs in two phases, a lag phase in which Tha4 assembles with the precursor protein-bound receptor complex, followed by a transport phase (Mori and Cline, 2002). Tha4

assembles reversibly; it is completely disassembled by the end of the transport phase and will reassemble with additional precursor protein. In order to analyze transport characteristics, we conducted a variety of chase reactions of bound precursor proteins. Conceptually, the transport phase could proceed in two very different ways. In the simplest scenario, each binding site would be competent for Tha4 recruitment and transport. In this case, with sufficient Tha4, all bound precursor proteins would be transported independently. The rate of the transport phase would be governed by 1st order kinetics; i.e. rate =k*[precursor protein] and would be described by an exponential curve. On the other hand, transport of bound precursor proteins could proceed in a sequential fashion where only one site in the complex is active for transport at any time. This would be described by a different rate equation in which rate=k*[complexes with at least one bound precursor protein]. In the case of a precursor protein-saturated complex, transport rate in a sequential mode would be constant for an extended time until complexes were depleted of precursor protein.

To differentiate between these two possible modes of transport, chase kinetics of receptor bound precursor protein were analyzed with different sets of starting conditions that included ~20% precursor protein occupancy of binding sites vs. full occupancy, and a range of Tha4 concentrations from 7 Tha4 per precursor protein to 120 Tha4 per precursor protein, obtained by supplementing reactions with *in vitro* translated Tha4 (Dabney-Smith et al., 2003). Transport was scored by the appearance of the mature form of OE17 (mOE17; cleavage of the signal peptide). Two observations indicate that appearance of mOE17 accurately measures transport. Hashimoto et al. (1996) showed that the OE17 precursor is not processed until the entire protein is across the

membrane. Second, time course analysis in which reactions were terminated rapidly with $HgCl_2$ (Reed et al., 1990) showed that all transported proteins had been processed to mature form (data not shown). As shown in Fig. 3-8, in 3 of 4 different conditions (including one in which all sites were occupied), ~ 90 of the initially bound precursor protein was transported in 25 to 30 min, which is consistent with ~10% non-specific binding. This indicates that all binding sites are functional for transport.

The transport kinetics of these three cases exhibited a lag phase followed by an exponential phase. The data were best fit to a generic sigmoidal equation (Appendix Experimental Procedures). The transport phase was analyzed by subtracting the lag time in each chase (Appendix Experimental Procedures). In chase reactions where the Tha4 per precursor protein ratio was 25 or more, the transport phase was best fit to an exponential first order kinetic equation. Because of the differences in the absolute rate of transport for the different reactions, the data were plotted as % maximum transport on the same graph. The three curves could virtually be superimposed (Fig. 3-9) and yielded very similar k_{cat} values of ~0.3. This indicates that, regardless of the occupancy level of receptor complexes, with sufficient Tha4, all precursor protein-bound sites were independently competent for transport (Fig. 3-9, Table 3-1).

In one case, i.e. with saturated complexes, where the Tha4 per precursor protein ratio was only 7, the transport phase in the first 15 min was linear (i.e. constant rate), and then decreased to a lower rate. This suggests that 7 Tha4 per precursor protein is insufficient to functionally assemble in all sites at any one time, or in other words it can functionally assemble with a fraction of the occupied sites and recycles to new sites after each transport event (Fig. 3-9). If so, then a rough estimate of the fraction of sites

that were initially active in this case can be obtained from the ratio of maximum rates from parallel chases of precursor protein-saturated membranes with 7 Tha4 per precursor protein vs. 25 Tha4 per precursor protein (Fig 3-9, Table 3-1). A ratio of 0.28 indicates that 7 Tha4 per precursor is enough to productively assemble with 28% of the precursor-bound sites, meaning that the minimum functional size of the Tha4 oligomer per bound OE17 precursor is 7÷0.28=25.

The Minimal Tha4 Oligomer Required to Transport an OE17 Precursor has ~28 Protomers.

In order to better determine the minimum Tha4 oligomer per site, a series of chase reactions with precursor-saturated receptors was conducted (Fig. 3-10). The Tha4 per precursor protein ratio was varied by from 7 to 84 with *in vitro* translated Tha4. The chase data were fit to a sigmoidal model (Fig. 3-10 A) and the maximum transport rates determined from the first derivative of the curves (Fig. 3-10 B). When maximum rate was plotted vs. the Tha4 per precursor ratio (Fig. 3-10 C), chases with 20 to 84 Tha4 per precursor protein had nearly identical maximum rates as expected from the results in Fig.3-9. However, the rate linearly declined with the drop in ratio below 20 Tha4 per precursor. Analysis of the transport rate break point from three independent experiments gave an estimate of the minimum functional size of the Tha4 oligomer of 28 protomers (SD 6.9).

A slightly different experimental design was used as an alternative approach to the optimal Tha4 oligomer. Endogenous Tha4 was the only source employed and the range of Tha4/precursor protein was obtained by varying the amount of bound precursor protein (Fig. 3-11). The average minimal Tha4 size for two such experiments was ~ 47 Tha4 protomers. However, we think that this is an overestimate of the Tha4 that is

available to participate in the chase reaction. Subfractionation of chloroplasts showed that a significant amount of Tha4 is present in the envelope membranes (Fincher et al., 2003). Quantification of the Tha4 content of intact chloroplasts vs. purified thylakoids suggest that envelope bound Tha4 contributes ~35% of the total. Our chase reactions contain most of envelope present in intact chloroplasts (Appendix Experimental Procedures). In the chases supplemented with *in vitro* translated Tha4 (Fig. 3-10), the influence of the unavailable envelope localized Tha4 or any inactive endogenous was less important to the calculation. Therefore, we think that the estimation of the 28 Tha4 protomers per functional oligomer size is more accurate.

Our analysis of the kinetic data assumes that the assembly step in the transport reaction involves Tha4 diffusion to and organization at the transport site. Thus, the assembly phase should depend upon the Tha4 availability. A plot of the lag time of the transport reactions in the experiment shown Fig. 3-10 does correlate with Tha4/precursor protein. Interestingly, at low concentrations of Tha4, there is a direct inverse relationship in the duration of the assembly phase, and above the Tha4 oligomer minimal size, the lag time is independent of Tha4 concentration. A similar analysis of the experiment relying only on endogenous Tha4 indicates that the important factor is the ratio of Tha4/precursor and not the Tha4 concentration in the membranes (Fig. 3-11 B). Although the lag times in Fig. 3-10 are slightly longer than those showed in Fig 3-8, Table 3-1, both experiments suggest that there is a Tha4 concentration independent step in the assembly phase.

Discussion

This study addressed the stoichiometry of precursor protein binding to the cpTat receptor complex and explored the implications for the transport mechanism. We

previously showed that at least four precursor proteins can bind independently to a single cpTat complex and form tetramers by disulfide crosslinking (Ma and Cline, 2010). Bound tetramers were subsequently transported as an oligomer, arguing for a complex with at least 4 binding sites. In the present work, we found that each cpTatC binds a precursor protein, suggesting that each receptor complex has 7 to 8 binding sites. Analysis of the transport step showed that all precursor protein bound-receptor sites can function independently for transport and, furthermore, suggested a minimal Tha4 oligomer size of 28 protomers for transporting an OE17 precursor protein. Thus, for the OE17 precursor, a functional Tat translocase unit consists of one TatC (one Hcf106) and ~28 Tha4.

The ratio of precursor protein per cpTatC was determined with three different methods, each with advantages and disadvantages. Binding saturation assays are the most direct measurement of binding stoichiometry at saturation. However, they may overestimate the ratio of precursor protein per cpTatC if non-specific binding is underestimated. The second approach, increase in binding after importing precpTatC, is not affected by non-specific binding but assumes that all imported cpTatC is functional. The third approach, immunopurification of detergent solubilized complexes, eliminates the contribution of the lipid bilayer and other membrane proteins to non-specific binding, but is subject to any instability of the precursor-bound receptor complex. The fact that these three different approaches gave remarkably similar ratios indicates that these potential problems are minimal. The number of cpTatC-Hcf106 per receptor complex is an estimate based on analysis of detergent solubilized receptor complexes. The thylakoid receptor complex contains only cpTatC and Hcf106 (Mori and Cline,

unpublished) and migrates on BN-PAGE at 700 kDa. Membrane proteins generally migrate on BN-PAGE at 180% of the actual molecular weight due to contribution of bound Coomassie Brilliant Blue (Heuberger et al., 2002). Thus, the corrected molecular weight divided by the combined molecular weight of cpTatC plus Hcf106 suggests ~7.5 heterodimers per complex, which is remarkable similar to the structural studies of Tarry et al. (2009).

On the other hand, our binding stoichiometry is much greater than that reported by Tarry et al. (2009) for the isolated *E coli* TatBC receptor complex. They observed complexes containing 0, 1, or 2 bound pre-SufI precursor proteins. Interestingly, when two precursor proteins were bound, they were always found in adjacent positions separated by ~50° with respect to the center of the TatBC complex, a geometry that suggests 7 potential binding sites per complex. The most likely explanation for the difference between our results and those of Tarry is that preSufI progressively dissociated during purification. In fact, we found that electrophoresis of the digitonin-solubilized thylakoid complex on BN-PAGE yielded a complex with a stoichiometry of 0.2:1 precursor proteins per cpTatC, as the apparent result of dissociation during electrophoresis. Thus, the stoichiometry obtained for detergent solubilized and purified receptor complexes will depend on the harshness of the method and on the affinity and rate of dissociation of each particular precursor protein for the binding site. Consistent with this interpretation, a previous study of bound OE17 precursor proteins that were additionally stabilized by disulfide crosslinking to tetramers, reported that the precursor protein bound receptor complex migrated on BN-PAGE at ~800 kDa (Ma and Cline, 2010). In the case of the OE17 precursor protein used here, which had a Kd of ~1 nM

and very slow dissociation at 4°C, more gentle manipulations, e.g. metal affinity chromatography, did not affect the ratio of precursor protein to cpTatC in solubilized complexes. However, it is not surprising that complexes isolated by Tarry (2009) had a much lower stoichiometry, considering that the precursors used have apparent Kd values of 50 to 100 nM.

Multivalent receptors frequently exhibit cooperativity, wherein binding to one site alters the affinity of other sites in the complex. The issue of cooperativity for the Tat transport system has been a matter of debate. A study with thylakoid membranes suggested that cpTat displays positive cooperativity for transport (Alder and Theg, 2003b) but did not differentiate between cooperativity at the binding or translocation step. Tarry et al. (2009) argued for a negative binding cooperativity for the *E coli* Tat system to explain the fact that TatBC complexes contained only one or two bound precursor proteins. In the present study, analysis of binding data gave a Hill coefficient of ~1, indicating that there is no cooperativity of binding. This was true even when binding points in the middle range between low occupancy and saturation were analyzed, where cooperativity is most likely to be detected. We interpret these data to indicate that binding sites are completely independent. The implication of this finding, i.e. that precursor proteins randomly bind to sites on the receptor complex, is currently under investigation.

Transport of bound precursor proteins upon energizing thylakoid membranes involves assembly of a Tha4 oligomer with the precursor protein-bound receptor. Previous work characterized Tha4 assembly as an essential step and correlated Tha4 assembly with a lag phase before transport begins (Mori and Cline, 2002). Here, we

confirmed that transport of bound precursor protein involves two steps and further showed that the relative abundance of Tha4 in the membrane is inversely proportional to the lag time when the Tha4 concentration is limiting. We also found evidence that the assembly step includes a Tha4 concentration independent event, possibly related to Tha4 polymerization and conformational changes upon docking with the receptor complex.

Analysis of the transport phase of the chase reaction (Figs. 3-9, 3-10, and 3-11) gave considerable insight into the Tha4 requirement for the transport mechanism. Below a Tha4/precursor protein ratio of ~28, the maximum rate increased linearly with increasing ratio. Above a ratio of 28, the maximum transport rate was constant. Importantly the rate of transport at all levels above ~28 obeyed first order kinetics with comparable k_{cat} values. This was true regardless of the occupancy level of the receptor complex. This latter observation supports our interpretation that all precursor bound sites are independently functional for transport, and that, with sufficient Tha4, can transport simultaneously. The efficient transport of crosslinked tetrameric precursor proteins, each bound to a receptor site (Ma and Cline, 2010), provides independent support for that conclusion and even suggests that adjacent sites can collaborate for transport of an oligomer.

Two other insights into mechanism could be gleaned from analysis of chase reactions. The first is the relative sluggishness of the translocation step. Under conditions of Tha4 excess, the rate is determined primarily by the translocation step. The k_{cat} for transport was ~0.3 min^{-1}, meaning that it takes ~3 min to transport a 20 kDa precursor protein. This is significantly longer than the 20 seconds that it takes to

transport the 37 kDa proOmpA by the *E. coli* SecA/SecYEG machinery (Liang et al., 2009). Some of the difference may be due to the fact that our assays were conducted at 15°C vs. the Sec assays at 37°C. However it is important to note that both temperatures are physiological temperatures for the respective organism, i.e. pea plants are grown at 16°C. Current views are that transport of proteins by the Sec apparatus consists of processive feeding of 25 residue segments of the unfolded precursor protein through the SecYEG channel, with each step driven by the ATPase activity and conformational changes of SecA. There are two models for the translocation step of Tat systems. One is that Tha4 (TatA) assembles appropriately sized oligomeric channels through which the bound precursor protein crosses to the trans side of the membrane (Gohlke et al., 2005; Leake et al., 2008). Another is that Tha4 (TatA) assembles oligomers at the site of the bound precursor protein that facilitate precursor protein transport by destabilizing the membrane bilayer (Bruser and Sanders, 2003). Although not strongly favoring either model, the sluggish transport step reported here does seem more consistent with facilitated movement through the bilayer than with transport through an appropriately sized channel.

The second insight into Tat mechanism concerns the functional size of the Tha4 oligomer. Much speculation has centered on the size and arrangement of Tha4 (TatA) at the translocation site. Initial channel models were proposed based on the molar ratio of endogenous Tat components (Berks et al., 2000). Although this has been dismissed in a recent report of far fewer Tha4 in *Arabidopsis* thylakoids than expected for a channel, (Jakob et al., 2009), this analysis may have underestimated the content due to the nature of the quantification method and the fact that Tha4 appears tenuously bound

to thylakoids. Several analyses of detergent solubilized TatA (Tha4) have made conclusions regarding the functional size and arrangements of TatA (Tha4) (Gohlke et al., 2005). However *in vivo* imaging experiments indicate that detergent-solubilized preparations do not accurately represent the situation in the membrane (Leake et al., 2008). Recent studies have obtained size estimates that are more closely correlated with the transport reaction. Dabney-Smith, et al. (2009), suggested, based on Cys-Cys disulfide crosslinking, that Tha4 is present as tetramers when not involved in transport and as oligomers of at least 18 Tha4 protomers when involved in transport. Leake, et al. (2008), with *in vivo* imaging of TatA-YFP, also suggested that TatA is tetrameric when not transporting and can be observed as spots that range in size from 4 to 100 with a median size of 25 TatA when in an actively transporting bacterium. Thus one model that is gaining favor is called the polymerization model, where Tha4 (TatA) tetramers would polymerize at precursor bound receptor sites until a large enough oligomer for translocation is achieved; at which point the precursor is transported.

One limitation of the Cys-Cys crosslinking estimate (Dabney-Smith and Cline, 2009) and the *in vivo* imaging estimate (Leake et al., 2008) is that it was unclear whether the presumed oligomers was associated with one or more translocating precursor proteins. Here we took a different approach to determine the functional size of the Tha4 oligomer for a single translocating protein; we measured the minimal amount of Tha4 required to activate all precursor bound sites in the membrane for transport. By analyzing kinetics of a series of chase reactions in which all binding sites were occupied, we found a biphasic response to increasing levels of Tha4. Below the break point in the curve, maximum transport linearly increased with the Tha4 per precursor

protein ratio; above the break, maximum transport rate was constant and independent of additional Tha4. The break in the curve is most easily interpreted to mean that Tha4 is sufficient for optimal transport at the break point. And the break point average for three such experiments was 28 ± 6.9 Tha4 protomers for each OE17 precursor. This number is tantalizing to view in the context of models for Tat transport. Gohlke et al. (2005) used single particle images of TatA complexes to estimate that 19 TatA protomers would provide a channel with 30-35 Å diameter, sufficient for the OE17 precursor. At present, there is no way to know how many Tha4 would be required to destabilize the bilayer for translocation. Clearly, a better determination of the factors that influence optimal size is required. Among them are precursor size, specific targeting sequence, temperature, etc. The experiments described here provide a method for achieving that goal.

In conclusion, the studies reported here for binding and transport indicate that for the OE17 precursor protein, a minimal Tat translocation unit consists of one cpTatC, one Hcf106, and 28 Tha4. This is an important advance in understanding the mechanism by which this unusual transport system can transport fully folded proteins across sealed membranes. However, these studies also raise a number of questions. For example, if Tha4 assembles as tetramers and polymerizes, then in the case where Tha4 is insufficient to activate all precursor-bound sites, there must be considerable dynamics of recruited Tha4 among sites to reach a functional size of the oligomer at any site. Without a dynamic exchange of Tha4 tetramers among precursor occupied sites, there would be no transport when falling substantially below the quantity of Tha4 required to activate all precursor bound sites. However, that doesn't seem occur (Figs

3-9, 3-10 and 3-11). Another question raised by our studies is how the Tha4 oligomer disassembles from one site and moves to another site. An efficient mode of doing this would be for the oligomer to simply move to an adjacent occupied site without disassembling into tetramers. Such a mechanism would provide an efficiency advantage for organizing non-interactive receptor units into a large multivalent receptor complex.

Table 3-1. Chase kinetic parameters

Chase	Receptor occupancy (%)	Tha4/precursor (mol/mol)	Lag time (min)	Max rate (%/min)	k_{cat} (min^{-1})	Precursor half-life ($t_{1/2}$) (min)
Chase 1	100	7	1.3	5	NA	NA
Chase 2	100	25	0.8	23	0.24	2.89
Chase 3	20	40	1.3	24	0.29	2.39
Chase 4	20	120	0.4	26	0.32	2.16

Table 3-2. Minimal Tha4 oligomer size

Chase	Receptor occupancy (%)	Tha4/precursor (molec/molec)	Lag time (min)	Max rate (%/min)	Fraction of active sites	Functional Tha4 oligomer estimate (molec)
Chase 1	100	84	1.5	12.3	1.00	NA
Chase 2	100	65	1.5	13.3	1.00	NA
Chase 3	100	22	1.7	13.0	1.00	NA
Chase 4	100	20	1.6	11.7	0.91	22.1
Chase 5	100	15	2.0	10.9	0.85	17.5
Chase 6	100	12	2.4	7.1	0.55	21.8
Chase 7	100	7	3.1	3.0	0.23	28.6

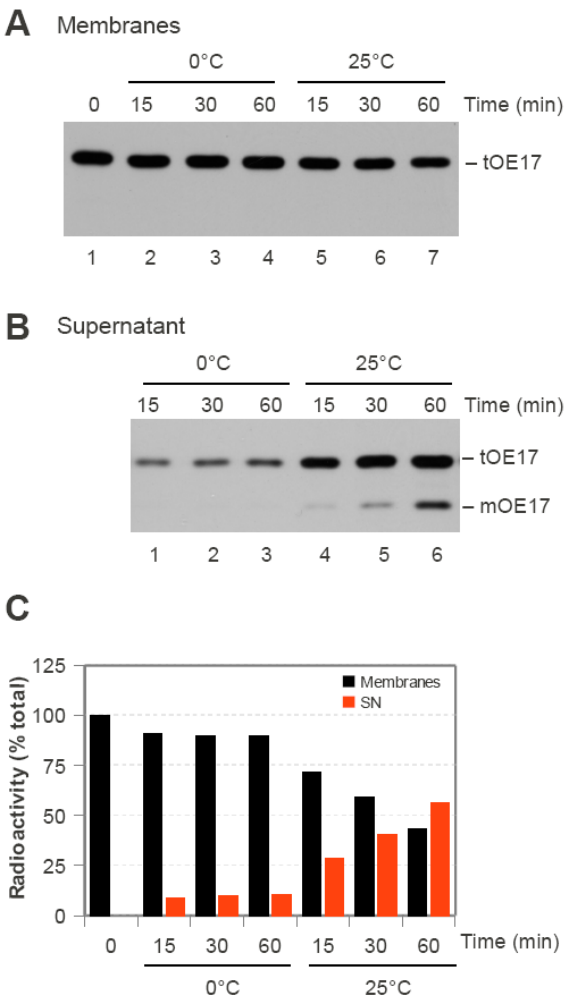

Figure 3-1. Precursor proteins bind with high affinity to the receptor complex and cannot be easily displaced. Thylakoid membranes were incubated with saturating amounts of radiolabeled precursor as described in Appendix Experimental Procedures. After binding, membranes were washed twice and then incubated with saturating amounts of unlabeled precursor at two temperatures: 0°C and 25°C. At time points, aliquots were removed and centrifuged. Membranes (A) and supernatant (B) fractions for each time point were analyzed by SDS-PAGE and fluorography. Radioactivity was measured by scintillation counting and plotted as percent of total for each time point (C).

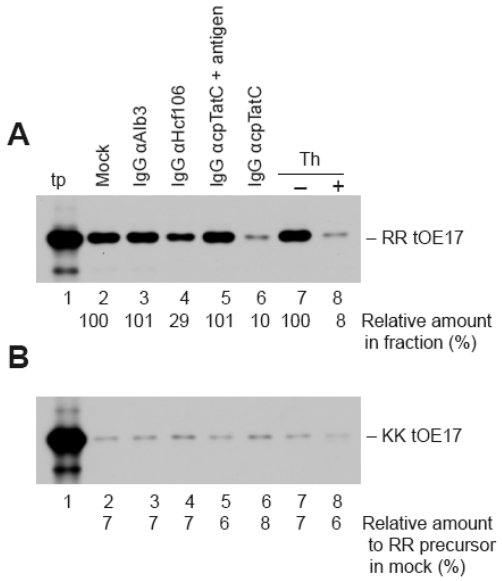

Figure 3-2. Precursors bind directly and specifically to cpTatC. Thylakoid membranes were treated with 0.5 mg/ml IgGs (lanes 3 to 6) in the absence or presence of antigen (lane 5) for 1 h on ice and then incubated with saturating amounts of radiolabeled precursor, RR tOE17 (A) or KK tOE17 (B). Alternatively, thylakoids were treated or mock treated with 100 µg/ml thermolysin (lanes 7 and 8) for 40 min on ice. Proteolysis was terminated with EDTA after which membranes were recovered, washed with IB 5 mM EDTA, and then incubated with saturating amounts of radiolabeled precursor, RR tOE17 (A) or KK tOE17 (B). After 1 h incubation with precursor, membranes were recovered by centrifugation, washed twice and resuspended in IBM buffer. Samples were analyzed by SDS-PAGE and fluorography as described in Appendix Experimental Procedures.

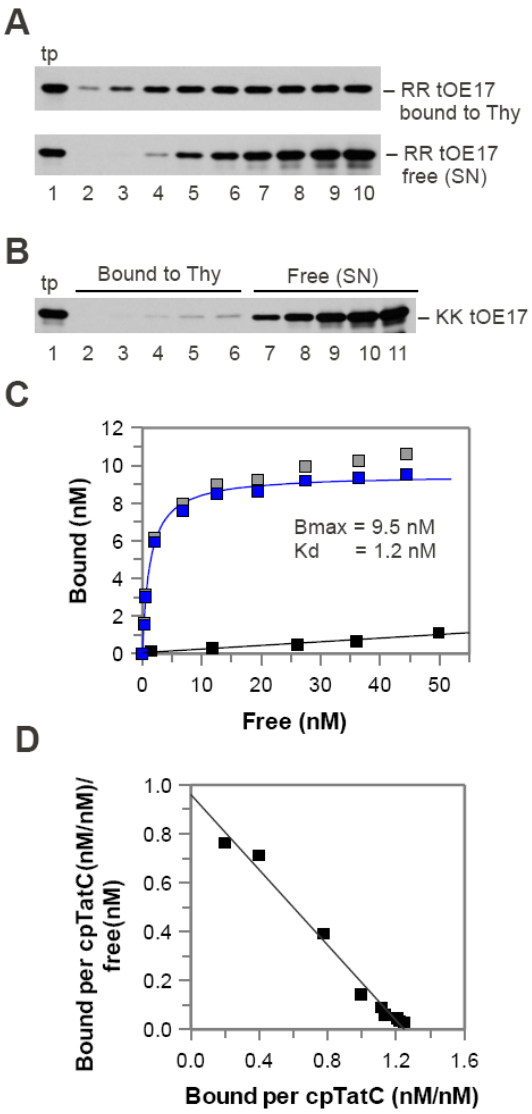

Figure 3-3. Binding saturation assay in thylakoid membranes. (A) Increasing amounts of radiolabeled RR tOE17 were incubated with washed thylakoids for 1 h at 4°C in a binding reaction as described in Appendix Experimental Procedures. Membranes recovered after binding were used to quantify bound precursor (A, upper panel) and the supernatant after binding to quantify free unbound precursor (A, lower panel). (B) Nonspecific binding was estimated in a parallel binding assay with a nonfunctional KK tOE17. (C) Total bound precursor (grey), non-specific binding (black) and total minus nonspecific binding (blue) were plotted against free unbound precursor. Specific binding was fitted to a single binding site model (solid blue line). (D) Scatchard analysis.

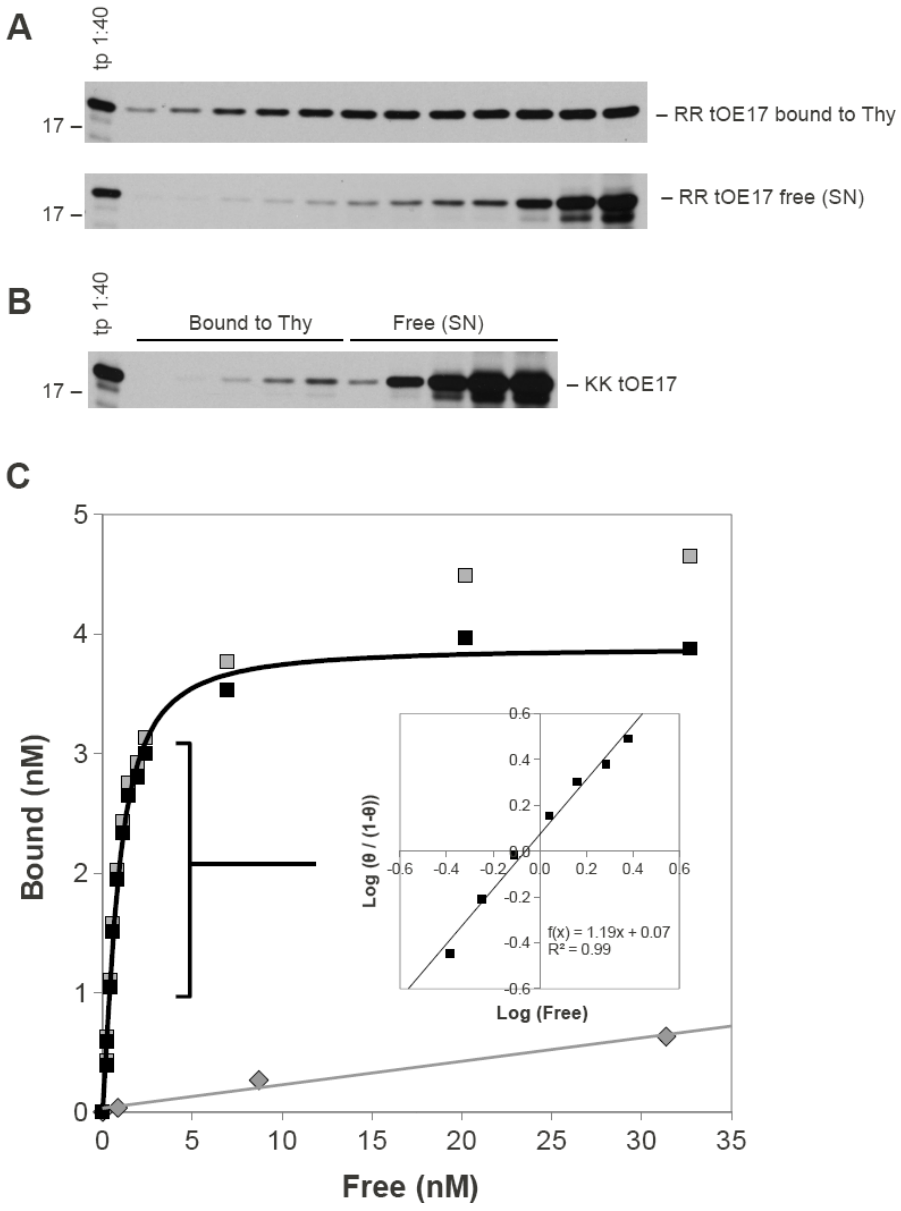

Figure 3-4. Hill slope analysis indicates independent binding sites in the receptor complex. Increasing amounts of radiolabeled RR tOE17 precursor were incubated with thylakoid membranes for 1 h at 4°C in a binding reaction. The amounts of precursor for each binding reaction were chosen to have several points in the middle region of the curve. Membranes were recovered by centrifugation and washed twice with IBM. Samples were analyzed by SDS-PAGE and fluorography as described in Appendix Experimental Procedures. (A, upper panel) precursor bound to thylakoids. The supernatant after binding was used to quantify free unbound precursor in the reaction (A, lower panel). (B) non-specific binding (gray diamonds) and total minus non-specific binding (black squares) were plotted versus free unbound precursor and fitted to a single binding site model. Hill plot for the middle region points in the curve (inset in C)

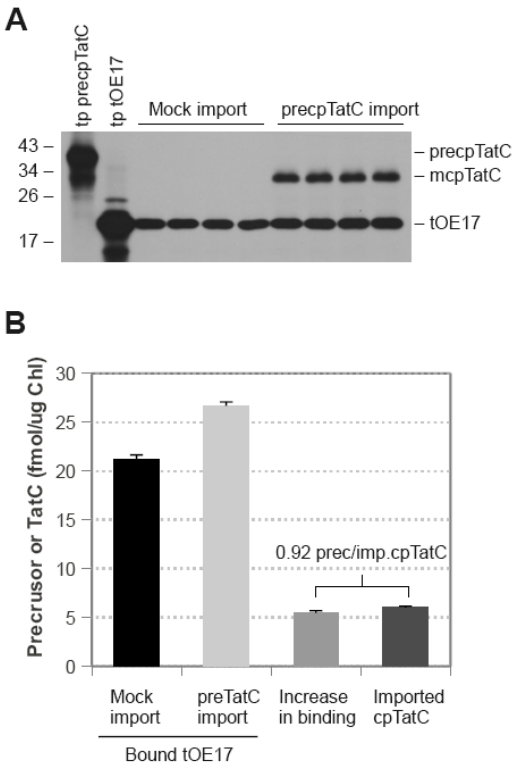

Figure 3-5. Import of cpTatC into chloroplasts increases thylakoid binding capacity by ~1 precursor per imported cpTatC. (A) preTatC and mock import reactions were each performed in 4 replicates for 1 hour as described in Appendix Experimental Procedures. Chloroplasts were repurified after import and treated with thermolysin for 40 min on ice previous to thylakoid isolation. Radiolabeled tOE17 was added to mock-import and to preTatC-import thylakoids and incubated in a binding reaction as described in Appendix Experimental Procedures. (B) Radiolabeled imported cpTatC and precursor were quantified by scintillation counting and plotted. Increase in binding was obtained as the difference in the amount of bound precursor between thylakoids with imported cpTatC and mock import thylakoids. Error bars represent the mean ± SD, n = 4.

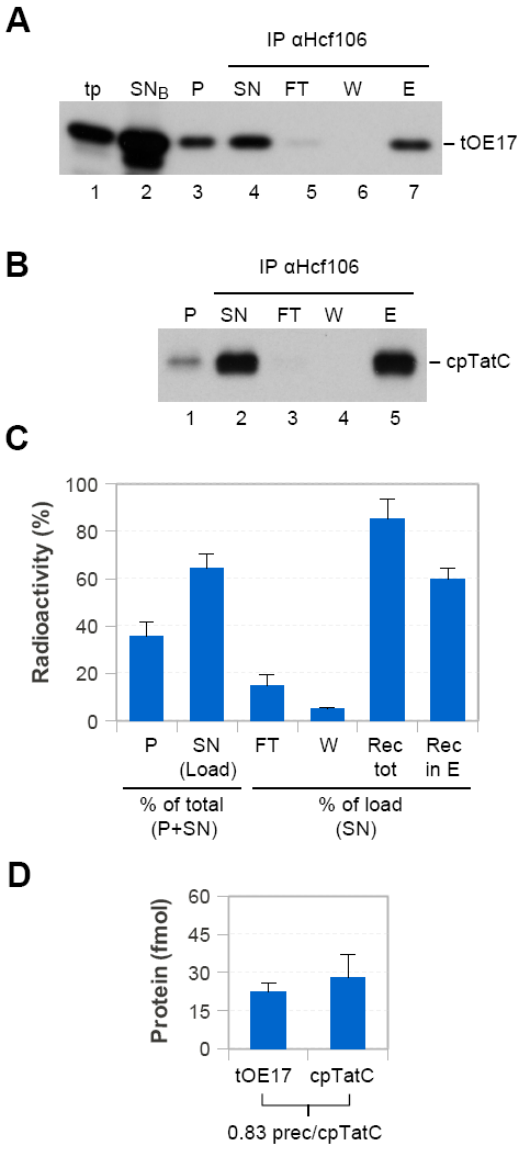

Figure 3-6. Immunopurified precursor bound receptor complex contains ~1 precursor per cpTatC. Thylakoids were incubated with saturating amounts of precursor in a binding reaction as described in Appendix Experimental Procedures. Precursor bound thylakoids were solubilized with digitonin and the insoluble pellet (lanes P) removed by centrifugation. The supernatant (lanes SN) was incubated with Hcf106 IgG beads (Appendix Experimental Procedures) and the unbound material (lanes FT) removed following centrifugation. The recovered beads were washed (lanes W) and then eluted (lanes E) with SDS buffer containing urea. (A) Precursor recovered in fractions. (B) cpTatC in fractions as determined by immunoblotting. (C) Precursor was quantified by scintillation counting in each fraction and displayed as percentage of starting material. (D) Precursor and cpTatC were quantified in the elution as described in Appendix Experimental Procedures. Error bars represent the mean ± SD, *n* = 3.

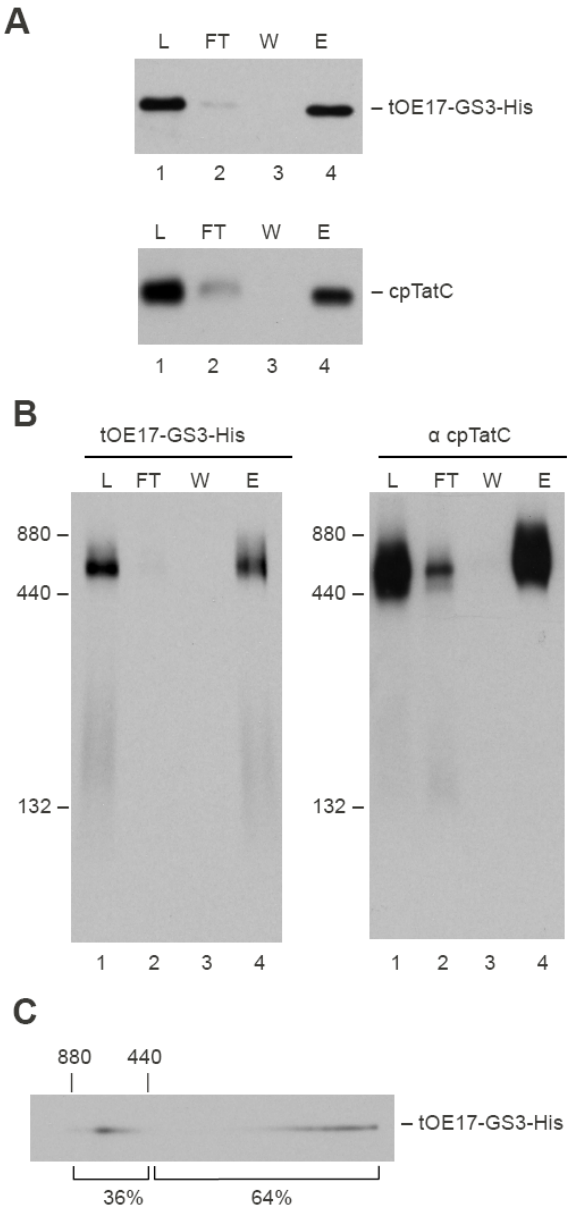

Figure 3-7. Bound precursors are dissociated from the receptor complex during electrophoresis on BN-PAGE. Saturating amounts of His tagged precursor were incubated with thylakoids in a binding reaction. The recovered and washed thylakoids were solubilized with digitonin as described in Appendix Experimental Procedures. Solubilized membranes (lanes L) were incubated with Ni-NTA magnetic beads purified for metal ion affinity purification and the unbound fraction (lanes FT) removed after magnetic separation. The beads were washed (lanes W) and then eluted with EDTA (lanes E) and analyzed by SDS-PAGE (A) and BN-PAGE (B). Second dimension analysis of the BN-PAGE lane L (C). The radioactivity in the second dimension gel was quantified separately for the receptor complex band (880-440 kDa) and below, and displayed as percentage of total.

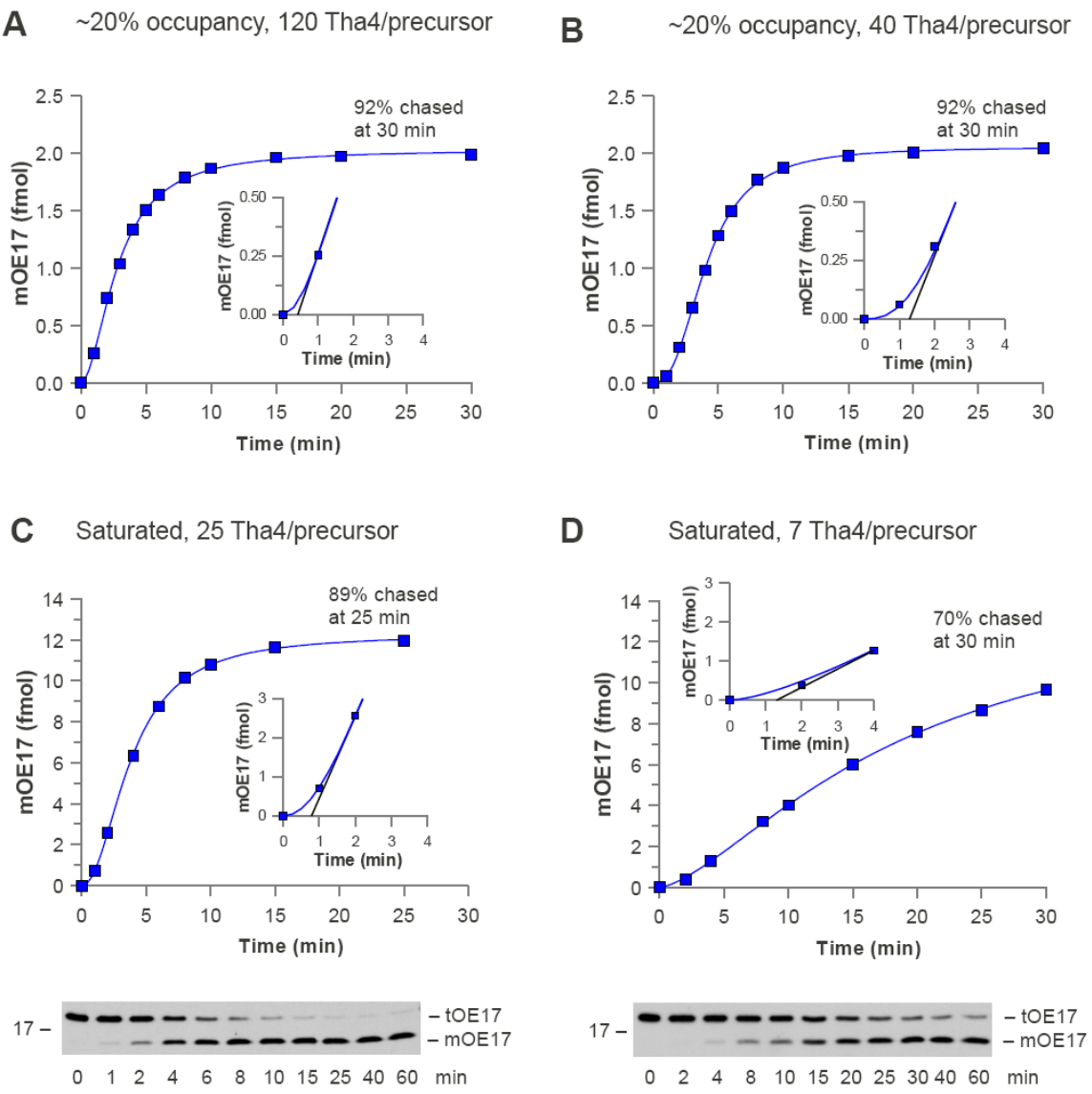

Figure 3-8. Chase kinetics in low occupancy and precursor-saturated thylakoid membranes with sufficient and insufficient Tha4.Thylakoid membranes were incubated in binding reactions with concentrations of precursor that resulted in 20% (A and B) or 100% (C and D) saturation of the receptor complexes. After binding, thylakoids were incubated with *in vitro* translated Tha4 (A and C) or mock translation (B and D) on ice for 20 min to allow Tha4 integration. Transport of bound precursor (chase) was initiated by addition of ATP and transfer to an illuminated bath at 15°C. Samples were removed at the designated times and analyzed as described in Appendix Experimental Procedures. The transported OE17 (mOE17) was fit to a generic sigmoidal equation (blue lines) (Appendix Experimental Procedures).Lag times were determined by the tangent method as described in Appendix Experimental Procedures (insets). Fluorograms of the chase reactions in C and D are displayed below the panels.

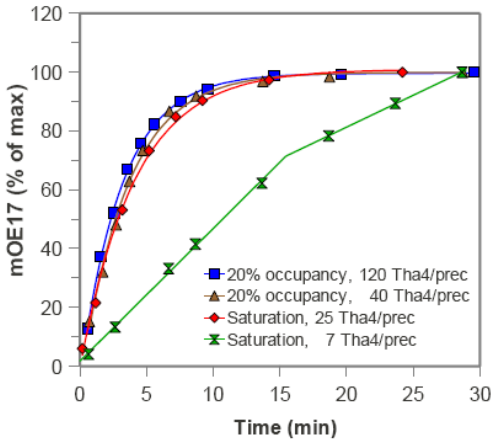

Figure 3-9. Analysis of the transport phase in lag-subtracted chase reactions. The lag time from each chase experiment shown in Fig. 7 was estimated as described in Appendix Experimental Procedures, and subtracted from each time point. The resulting data were plotted as percent of maximum transport and fitted to an exponential first order equation.

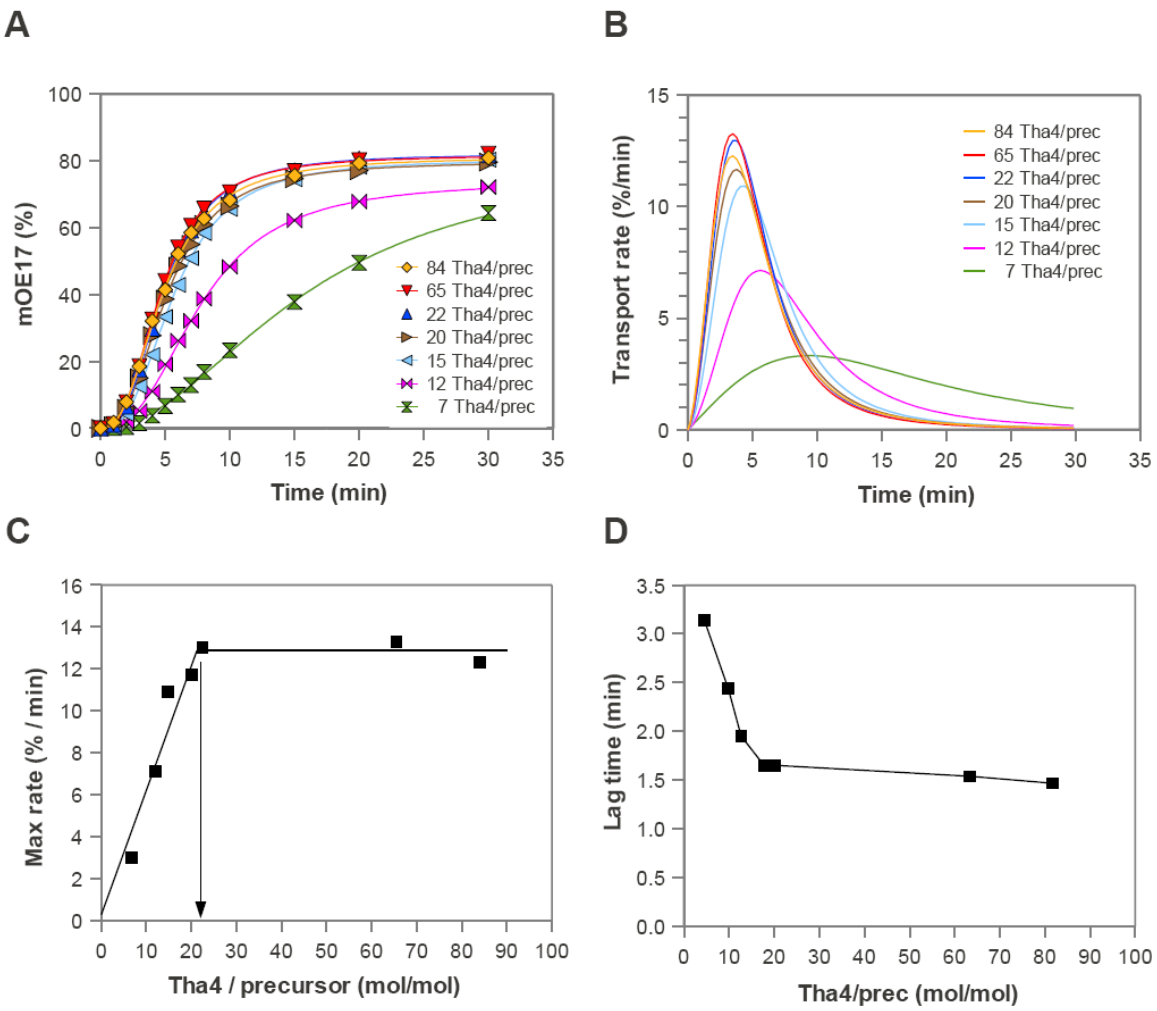

Figure 3-10. Tha4 oligomer minimal size. Chase reactions with precursor saturated membranes were conducted with different amounts of *in vitro* translated Tha4 as explained in Appendix Experimental Procedures. Chases were plotted as percent of time zero and fitted to a generic sigmoidal equation (A). Transport rates for each chase were estimated with the first derivative of the fitted curves (B). The amount of Tha4 per precursor was estimated for each chase as described in Appendix Experimental Procedures, and plotted versus maximum transport rates (C). A regression line for the four chases with <25 Tha4 per precursor is shown. A line of the average max rate for the three chases with higher rates is shown. The intercept of the two lines (arrow) indicates in the x-axis the minimal size of the Tha4 oligomer (21 Tha4 per precursor). Lag times were estimated as described in Appendix Experimental Procedures and plotted versus the ratio of Tha4/precursor.

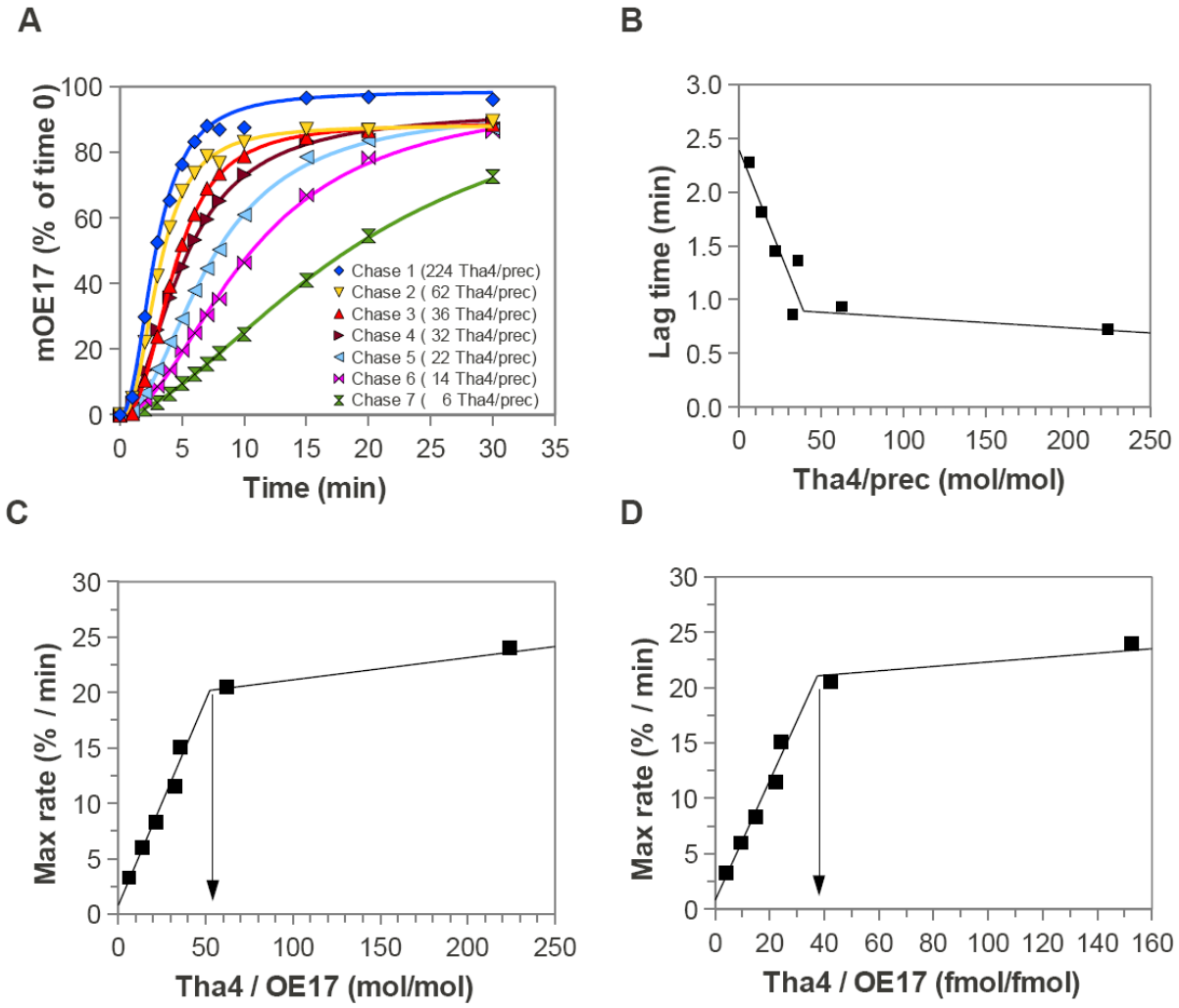

Figure 3-11. Tha4 oligomer minimal size estimated with endogenous Tha4. Chase reactions with increasing amounts of precursor were conducted as explained in Fig 3-10 except that no Tha4 was added to the reaction. Chases were plotted as percent of time zero and fitted to a generic sigmoidal equation (A). Transport rates for each chase were estimated with the first derivative of the fitted curves (data not shown). Lag times were estimated as described in Appendix Experimental Procedures and plotted versus the ratio of Tha4/precursor (B). The amount of Tha4 per precursor was estimated for each chase as described in Appendix Experimental Procedures, and plotted versus maximum transport rates (C). Envelope localized Tha4 was subtracted from the total amount and plotted versus maximum transport rates (D) A regression line for the five chases with lower rates is shown (C and D). A regression line for the two chases with higher transport rates is shown (C and D). The intercept of the two lines (arrow) indicates in the x-axis the minimal size of the Tha4 oligomer (51 Tha4 per precursor in C, and 37 Tha4 per precursor in D).

CHAPTER 4
SUMMARY AND CONCLUSIONS

In these studies we developed a novel quantitative immunoblotting method that allows an accurate quantification of low abundance membrane proteins in complex systems. Proof-of-concept experiments indicated an error in the quantification that varied between 5 to 8%. The accuracy of the method relies on using full-length standard proteins obtained by *in vitro* translation and correction factors for gel extraction efficiencies. Importantly, once the correction factors are determined, the method can be performed in a routine basis and is inexpensive. This method can be used in mechanistic studies to describe the number of binding sites in a receptor and identify cooperativity between binding sites. Reorganization of membrane protein complexes can also be studied by placing affinity tags in one of the complex components. Finally, when combined with a kinetic assay, this method can be used to estimate the stoichiometry requirements for enzyme activity in native membranes.

Two fundamental questions about the mechanism of protein transport by the twin arginine translocation (Tat) system were addressed in these studies: (1) the number of precursor binding sites in the Tat receptor complex and (2) the minimal size of the Tha4 homo-oligomer. Three different experimental approaches showed that each cpTatC binds one precursor protein, indicating that each receptor complex can bind 7-8 precursors. Analysis of transport reactions from the bound-state (chase) under different receptor occupancy levels and different amounts of Tha4, suggested that transport is independent at each binding site and that the minimal size of the Tha4 oligomer for the OE17 precursor is ~28 protomers. Analysis of the lag phase in chase reactions showed

an inverse linear relationship between lag time and the ratio of Tha4 per precursor below the minimal Tha4 oligomer size. Furthermore, we also found evidence that the assembly step includes a Tha4 concentration independent event which could be related to Tha4 polymerization or conformational changes. Analysis of the transport phase of membranes with sufficient Tha4 to activate all sites indicated k_{cat} values of ~0.3 min^{-1} that did not vary with receptor occupancy.

The multivalent nature of the Tat receptor complex and the capability of each binding site to independently recruit a Tha4 oligomer and transport a bound precursor, revealed novel and interesting aspects of Tat protein transport and at the same time opened new questions. Since precursor binding is non-cooperative, the reason for having multiple binding sites in the receptor complex is not completely clear at this point. One possibility is that oligomeric precursor proteins, each bearing a signal peptide, could be coordinately transported across the membrane as it was shown by Ma and Cline (2010). Tha4 recruitment at each binding site would facilitate assembly of a Tha4 oligomer large enough to transport oligomeric precursor proteins.

Currently, there are two models of how Tha4 could facilitate precursor translocation. One model proposes that Tha4 exists as a collection of oligomeric channels of different sizes that can be recruited to a precursor bound receptor complex. Precursor translocation would occur when the size of the Tha4 channel fits the size of the folded precursor. The second model proposes that Tha4 oligomers destabilize the membrane upon assembly with a precursor bound receptor complex and facilitate precursor transport. The results of these studies do not strongly support one model more than the other; however, the low k_{cat} values reported seem more consistent with a

facilitated movement through the bilayer than transport by an appropriately sized channel.

From the two existing models for Tat translocation, one could predict that larger precursors would require a larger Tha4 oligomer to be transported. Future studies should use the chase kinetics approach shown here to test the effect of precursor size in the rate of protein transport and in the Tha4 requirement to activate all binding sites. Other variables that would be interesting to study using a chase kinetics approach are precursor isoelectric point and reaction temperature.

APPENDIX
EXPERIMENTAL PROCEDURES

Source Plants, Chloroplasts and Thylakoid Isolation

Intact chloroplasts were isolated from 9 to 10-day-old pea seedlings, Progress #9 Improved, following published procedures (Cline et al., 1993). Chloroplasts were resuspended to 1 mg chlorophyll/ml in import buffer (330 mM sorbitol, 50 mM HEPES-KOH, pH 8.0) and kept on ice until use. Isolated thylakoids were obtained from intact chloroplast by osmotic lysis. Chloroplast pellets were lysed at 2 mg chlorophyll/ml in 10 mM HEPES-KOH, pH 8.0, containing 10 mM $MgCl_2$ at 0°C for 5 min and adjusted to import buffer, 10 mM $MgCl_2$. Thylakoids were obtained from lysates by centrifugation at 3,300 X *g* for 8 min and washing with IB, 5 mM $MgCl_2$. Thylakoids were resuspended to 1 mg chlorophyll/ml in IB, 5 mM $MgCl_2$ before use. Chlorophyll concentrations were determined according to Arnon (1949).

Plasmid Construction and Mutagenesis

Transcription clones for tOE17 V-20F (Gérard and Cline, 2007), preTatC and mTatC (Mori et al., 2001), and mTha4 (Fincher et al., 2003) are as described. The DNA clone for the His tagged precursor and His tagged mTatC were constructed by PCR mutagenesis using the QuickChange™ kit (Stratagene, La Jolla, CA) by adding an unstructured linker consisting of 3 GGGGS repeats and 6 histidine residues at the C-terminus of the protein. DNA sequencing on both strands at the University of Florida Interdisciplinary Center for Biotechnology Research DNA Sequencing Core Facility verified cloned constructs.

Preparation of Radiolabeled Precursors

Capped mRNAs were transcribed *in vitro* with SP6 polymerase (Promega) and were translated *in vitro* in the presence of [^{3}H]-leucine with a homemade wheat germ translation system (Cline, 1986). Translation was initiated by incubating translation mixtures at 25°C for 1 h and stopped by transferring to ice and adding 1 volume of 2X IB buffer containing 10 mM $MgCl_2$ and 400 µM cycloheximide.

Determination of Translation Product's Specific Radioactivity by Isotope Dilution Experiments

Isotope dilution experiments were used to determine the size of the unlabeled leucine pool in wheat germ extracts. In this determination, translation reactions contained 40% v/v of homemade wheat germ extract, and the following components at final concentrations in the assay: 1.5 mM ATP, 1.5 mM GTP, 38 µM unlabeled amino acids except leucine, 0.45 µCi/µl [^{3}H]-leucine (Perking Elmer), 12 mM phosphocreatine, 1.4 mM dithiotrietol, 77 µg/ml creatine phosphokinase, 1.9 mM MgOAc, 126 mM KOAc, 0.6 mM spermidine, 0.4 U/µl RNasin and mRNA. A series of translation reactions were carried out with increasing amounts of unlabeled leucine in a range from 0 to 80 µM final concentration. Translations were incubated at 25°C for 1 h and stopped by transferring to ice and adding 1 volume of 2X IB buffer, 400 µM cycloheximide. An aliquot of each translation received 1 volume of SDS sample buffer and was denatured at 37°C for 20 min. Translations were analyzed by SDS-PAGE and fluorography. Radiolabeled proteins were extracted from gel slices as described (Cline, 1986) and dpm were measured by liquid scintillation counting. The reciprocal of the radioactivity extracted from gel slices of radiolabeled proteins was plotted against total leucine concentration in the reaction (added unlabeled leu + [^{3}H]-leucine). The negative

intercept with the y-axis of the regression line obtained from the data points represents the concentration of endogenous unlabeled leucine contributed by the wheat germ extract (Patrick et al., 1989). The specific radioactivity of *in vitro* translated proteins was calculated by multiplying the ratio of [^{3}H]-leucine to total leucine in the translation reaction by the specific radioactivity of the [^{3}H]-leucine indicated by the manufacturer.

Scintillation Counting

In vitro translated proteins labeled with tritiatedleucine were measured by scintillation counting in a Beckman LS 6500. Counting efficiency for tritium and quench correction curves (chemical and color quench) were checked. A new counting efficiency correlation curve for tritium was generated with a set of PerkinElmer quenched standards. Counting efficiency for tritium was ~61%. The color quench correction system was specifically checked for chlorophyll by counting samples with the same amount of isotope and increasing amounts of chlorophyll. The counting accuracy of pigmented samples over a range of 0 to 6 μg chlorophyll was in average –2.7%.

Chloroplast Import and Thylakoid Protein Integration Assays

Radiolabeled precpTatC was incubated with isolated chloroplasts (0.33 mg chlorophyll/ml), 5 mM Mg-ATP in IB with 120 µE of light in a 25°C water bath for 30 min. After import, chloroplasts were pelleted and treated with thermolysin (100 µg/ml) for 40 min at 0°C. Protease treatment was stopped by adding EDTA to a final concentration of 8 mM. Intact chloroplasts were re-purified by centrifugation through a 35% percoll, 5 mM EDTA in IB. Recovered chloroplast were lysed hypotonically as described previously to separate stromal-intermediate cpTatC from thylakoid-integrated mcpTatC (Martin et al., 2009). Isolated thylakoids from import assays were washed once and resuspended to 1 mg chlorophyll/ml.

Integration of *in vitro* translated Hcf106 and Tha4 into isolated thylakoids was performed by incubating translation mixtures with washed thylakoids (0.5 mg chlorophyll/ml) at 25°C in the dark for 20 min. Following integration, membranes were washed twice with IB buffer, 5 mM $MgCl_2$, and resuspended to 1 mg chlorophyll/ml.

Precursor Binding

In vitro translated precursor proteins were treated with apyrase (10 U per 100 µl translation) for 30 min on ice to remove nucleosides. Binding reactions were performed by incubating apyrase-treated *in vitro* translated precursor proteins with isolated thylakoids in the dark at 4°C for 1 h. with end-over-end mixing. After binding, thylakoids were recovered by centrifugation, washed twice and resuspended to 1 mg chlorophyll/ml in IB, 5 mM $MgCl_2$.

Binding saturation data analysis

Specific binding curves were obtained by subtracting non-specific binding, determined with a KK precursor in a parallel assay, from total binding of the RR precursor protein. Specific binding data were fit by non-linear regression to a single site binding equation $B=B_{max}*[precursor]/(kd+[precursor])$ where B=concentration of bound precursor, [precursor]=concentration of free, unbound precursor, and the fitting parameters B_{max}= maximum binding, and kd=dissociation constant, using LabPlot-GNU software. The Hill coefficient in binding saturation assays was determined by fitting the data to a single site binding equation including a Hill slope term h ($B_{max}=B_{max}*[precursor]^h/(kd^h+[precursor]^h)$).

SDS-PAGE and Immunoblotting

Samples containing cpTatC, Hcf106 or Tha4 received 1 vol of sample buffer (4% SDS, 66% glycerol, 5% β-mercaptoethanol, 2 mM EDTA, 125 mM M Tris, pH 6.8) and

were incubated at 37°C for 20 min before electrophoresis to prevent cpTatC aggregation. Samples for SDS-PAGE analysis of precursor proteins were also mixed with sample buffer as before but heated at 95°C for 2 min. The acrylamide concentration in the gels was chosen to be the minimum required to resolve the protein being analyzed. The purpose of this was to facilitate electrophoretic transfer to blotting membranes and minimize gel retention. In this way, cpTatC and Hcf106 were analyzed in gels containing 9% acrylamide, and Tha4 in 12.5% acrylamide. Samples were loaded in gels with a syringe to prevent carry over. Gels were electroblotted on 0.2 µm pore-size polyvinylidine fluoride membranes for cpTatC and 0.2 µm pore-size nitrocellulose membranes for Hcf106 and Tha4. Before electroblotting, polyvinylidine fluoride membranes were wet in 100% methanol and then equilibrated in transfer buffer 20% methanol. Nitrocellulose membranes were directly equilibrated in transfer buffer 20% methanol. Electroblotting was performed in a wet tank system at 100 volts for 1 hour using transfer buffer (200 mM glycine, 25 mM Tris) containing 20% methanol. Blotted membranes were blocked for 25 min at room temperature in TBS-T buffer containing 5% fat-free milk with shaking. After blocking, membranes were rinsed twice with TBS-T and incubated with primary antibody for 1 h. with shacking. Blots were rinsed twice and washed for 25 min with three changes of buffer before secondary antibody decoration. Secondary antibody incubation was done for 1 h. with shacking. After washing the blots as before, antibody complexes were detected with the enhanced chemiluminescence method (ECL, GE Helathcare). Immunoblot films where scanned at 600 dpi in translucent mode using an Epson Perfection 3170 scanner. Scanned images were

analyzed by densitometry using Quantity One software (Bio-Rad). Gels were processed for fluorography as described (Bonner and Laskey, 1974).

Precursor Protein Chase Assay

For transport assays of thylakoid bound precursor protein (chase), 40 µg chlorophyll of thylakoids recovered from binding assays were further incubated with apyrase treated *in vitro* translated unlabeled mTha4 or mock translation extract on ice in the dark for 20 min. Following mTha4 integration, precursor protein-bound thylakoids received 1 volume of stromal extract and were equilibrated to 15°C in the dark for 5 min. Aliquots of the mixture were removed as time zero samples and for cpTatC quantification. The chase reaction was initiated with Mg-ATP (12 mM final concentration) and transfer to ~100 µmol/m^2/s white light at 15°C. At time points, aliquots were removed, mixed with SDS buffer and heated at 95°C for 3 min. Samples were analyzed by SDS-PAGE and fluorography.

Chase Kinetics Data Analysis

The amount of mature protein obtained for each time point was corrected for recovery and normalized to percent of time zero or percent of maximum transport as indicated. Normalized data were fit to a generic sigmoidal equation $y=a*x^b/(c^b+x^b)$ where y= mOE17, x= time , and a,b and c are fitting parameters, by nonlinear regression using the program Labplot-GNU. The maximum transport rate in a chase reaction was obtained with the 1^{st} derivative of the fitted sigmoidal curve by numerical differentiation using Labplot-GNU. The lag time for each reaction was estimated by the intercept with the x-axis of the tangent line to the fitted sigmoidal model at the point of maximum transport rate (Auer and Kashchiev, 2010). Lag times were subtracted from each time

point and the resulting data plotted and fitted to a first order exponential equation $y = a*e^{(-kcat*x)}+c$ where y= mOE17, x= time and k_{cat} is a fitting parameter.

Digitonin Solubilization

Thylakoid membranes were solubilized in 0.5% digitonin, 0.5 X IB, 20% glycerol, 0.5 M amino-caproic acid and 2 mM PMSF at 1 mg chlorophyll per ml for 1 h at 4°C with end-over-end mixing. Insoluble material was then collected by centrifugation at 150,000 x *g* at 2°C for 30 min and the supernatant removed to a new tube for further processing.

Blue Native Polyacrylamide Gel Electrophoresis

Thylakoids were solubilized with digitonin as described above and combined with 1:10 volume of 5% Coomassie Brilliant Blue G (Serva), 100 mM BisTris-HCl, pH 7.0, 0.5 M amino-caproic acid, 30% glycerol. BN-PAGE on 5-13.5% acrylamide gradient with 0.75-mm-thick gels and fluorography or immunoblotting were as described (Cline and Mori, 2001; Gérard and Cline, 2007). For 2D analysis, whole-lanes or bands between the 880 and 440 kDa markers were excised and soaked in 1X SDS sample buffer for 10 min at 37°C and were applied onto a 1-mm-thick SDS-PAGE.

Non-denaturing Immunoprecipitation

Thylakoids recovered from binding assays with saturating concentrations of precursor protein were solubilized with digitonin as described above except that the digitonin concentration was 1%. The 150,000 x g supernatant was incubated with protein A-Sepharose beads that had been cross-linked to Hcf106-IgG (Cline and Mori, 2001) for 2 hrs with end-over-end mixing at 4°C. Unbound proteins were recovered by centrifugation and the beads were washed with 0.5% digitonin, 0.5 X IB, 0.5 M amino-caproic acid, 20% glycerol for 10 min at 4°C. Bound proteins were recovered by

incubating the beads with 2X SDS, 8M urea, non-reducing sample buffer for 16 hrs at room temperature and removing the beads with a mini spin column (Promega).

Metal Affinity Purification under Non-denaturing Conditions

Washed precursor protein-bound thylakoids were solubilized with 0.5% digitonin as described above and the 150,000 x g supernatant combined with 1 volume 2X binding buffer (40 mM HEPES, pH 7.8, 300 mM NaCl, 40 mM Imidazole) and mixed with Ni-NTA magnetic agarose beads (Qiagen). The suspension was incubated at 4°C with end-over-end mixing for 8 hrs and unbound proteins recovered by removing the supernatant after 1 min in a magnetic rack. The beads were washed in 1X binding buffer, 0.25% digitonin for 2 min and bound proteins were eluted with 1X binding buffer 0.25% digitonin, 100 mM EDTA for 1 h with end-over-end mixing at 4°C. A second elution was performed with 2X SDS sample buffer containing 100 mM EDTA at room temperature for 1 h.

LIST OF REFERENCES

Alami, M., I. Lüke, S. Deitermann, G. Eisner, H.-G. Koch, J. Brunner, and M. Müller. 2003. Differential interactions between a twin-arginine signal peptide and its translocase in Escherichia coli. *Mol Cell*. 12:937-946.

Alder, N.N., and S.M. Theg. 2003a. Energetics of protein transport across biological membranes: a study of the thylakoid ΔpH-dependent/cpTat pathway. *Cell*. 112:231-242.

Alder, N.N., and S.M. Theg. 2003b. Protein transport via the cpTat pathway displays cooperativity and is stimulated by transport-incompetent substrate. *FEBS Lett*. 540:96-100.

Ali, M.H., and B. Imperiali. 2005. Protein oligomerization: how and why. *Bioorgan Med Chem*. 13:5013-5020.

Auer, S., and D. Kashchiev. 2010. Insight into the correlation between lag time and aggregation rate in the kinetics of protein aggregation. *Proteins*. 78:2412-2416.

Azevedo, J.E., and W. Schliebs. 2006. Pex14p, more than just a docking protein. *Biochim Biophys Acta*. 1763:1574-1584.

Balsera, M., T.A. Goetze, E. Kovács-Bogdán, P. Schürmann, R. Wagner, B.B. Buchanan, J. Soll, and B. Bölter. 2009. Characterization of Tic110, a channel-forming protein at the inner envelope membrane of chloroplasts, unveils a response to Ca(2+) and a stromal regulatory disulfide bridge. *J Biol Chem*. 284:2603-2616.

Barnidge, D.R., E.A. Dratz, T. Martin, L. Bonilla, L.B. Moran, and A. Lindall. 2003. Absolute quantification of the G protein-coupled receptor rhodopsin by LC/MS/MS using proteolysis product and synthetic peptide standards. *Anal Chem*. 75.

Bauer, M.F., C. Sirrenberg, W. Neupert, and M. Brunner. 1996. Role of Tim23 as voltage sensor and presequence receptor in protein import into mitochondria. *Cell*. 87:33-41.

Berks, B.C., T. Palmer, and F. Sargent. 2003. The Tat protein translocation pathway and its role in microbial physiology. *Adv Microb Physiol*. 47:187-254.

Berks, B.C., F. Sargent, and T. Palmer. 2000. The Tat protein export pathway. *Mol Microbiol*. 35:260-274.

Blobel, G., P. Walter, and R. Gilmore. 1980. Intracellular protein topogenesis. *Proc Natl Acad Sci USA*. 77:1496-1500.

Bohnsack, M.T., and E. Schleiff. 2010. The evolution of protein targeting and translocation systems. *Biochim Biophys Acta*. 1803:1115-1130.

Bolhuis, A., J.E. Mathers, J.D. Thomas, C.M.L. Barrett, and C. Robinson. 2001. TatB and TatC form a functional and structural unit of the twin-arginine translocase from Escherichia coli. *J Biol Chem*. 276:20213-20219.

Bonner, W., and R. Laskey. 1974. A film detection method for tritium-labelled proteins and nucleic acids in polyacrylamide gels. *Eur J Biochem*. 46:83-88.

Brocard, C., G. Lametschwandtner, R. Koudelka, and A. Hartig. 1997. Pex14p is a member of the protein linkage map of Pex5p. *EMBO J*. 16:5491-5500.

Bruser, T., and C. Sanders. 2003. An alternative model of the twin arginine translocation system. *Microbiol Res*. 158:7-17.

Carvalho, A.F., J. Costa-Rodrigues, I. Correia, J. Costa Pessoa, T.Q. Faria, C.L. Martins, M. Fransen, C. Sá-Miranda, and J.E. Azevedo. 2006. The N-terminal half of the peroxisomal cycling receptor Pex5p is a natively unfolded domain. *J Mol Biol*. 356:864-875.

Chacinska, A., C.M. Koehler, D. Milenkovic, T. Lithgow, and N. Pfanner. 2009. Importing mitochondrial proteins: machineries and mechanisms. *Cell*. 138:628-644.

Cline, K. 1986. Import of proteins into chloroplasts. *J Biol Chem*:14804-14810.

Cline, K., R. Henry, and C. Li. 1993. Multiple pathways for protein transport into or across the thylakoid membrane. *EMBO J*. 12:4105 - 4114.

Cline, K., and M. McCaffery. 2007. Evidence for a dynamic and transient pathway through the TAT protein transport machinery. *EMBO J*. 26:3039-3049.

Cline, K., and H. Mori. 2001. Thylakoid ΔpH-dependent precursor proteins bind to a cpTatC-Hcf106 complex before Tha4-dependent transport. *J Cell Biol*. 154:719-729.

Cline, K., and S.M. Theg. 2007. The Sec and Tat protein translocation pathways in chloroplasts. *In* The enzymes, molecular machines involved in protein transport across cellular membranes. Vol. 25. R.E. Dalbey, C.M. Koehler, and F. Tamanoi, editors. Elsevier, London:. 463-492.

Dabney-Smith, C., and K. Cline. 2009. Clustering of c-terminal stromal domains of Tha4 homo-oligomers during translocation by the Tat protein transport system. *Mol Biol Cell*. 20:2060 -2069.

Dabney-Smith, C., H. Mori, and K. Cline. 2003. Requirement of a Tha4-conserved transmembrane glutamate in thylakoid Tat translocase assembly revealed by biochemical complementation. *J Biol Chem*. 278:43027-43033.

Dabney-Smith, C., H. Mori, and K. Cline. 2006. Oligomers of Tha4 organize at the thylakoid Tat translocase during protein transport. *J Biol Chem*. 281:5476-5483.

Dolezal, P., V. Likic, J. Tachezy, and T. Lithgow. 2006. Evolution of the molecular machines for protein import into mitochondria. *Science*. 313:314-318.

Dyall, S.D., M.T. Brown, and P.J. Johnson. 2004. Ancient invasions: from endosymbionts to organelles. *Science*. 304:253-257.

Eckert, J.H., and N. Johnsson. 2003. Pex10p links the ubiquitin conjugating enzyme Pex4p to the protein import machinery of the peroxisome. *J Cell Sci*. 116:3623-3634.

Economou, A., and W. Wickner. 1994. SecA promotes preprotein translocation by undergoing ATP-driven cycles of membrane insertion and deinsertion. *Cell*. 78:835-843.

Fagerberg, L., K. Jonasson, G. von Heijne, M. Uhlen, and L. Berglund. 2010. Prediction of the human membrane proteome. *Proteomics*. 10:1141-1149.

Fincher, V., C. Dabney-Smith, and K. Cline. 2003. Functional assembly of thylakoid ΔpH-dependent/Tat protein transport pathway components in vitro. *Eur J Biochem*. 270:4930-4941.

Gakh, O., P. Cavadini, and G. Isaya. 2002. Mitochondrial processing peptidases. *Biochim Biophys Acta*. 1592:63-77.

Gerber, S.A., J. Rush, O. Stemman, M.W. Kirschner, and S.P. Gygi. 2003. Absolute quantification of proteins and phosphoproteins from cell lysates by tandem MS. *Proc Natl Acad Sci USA*. 100:6940-6945.

Gilmore, R., P. Walter, and G. Blobel. 1982. Protein translocation across the endoplasmic reticulum. II. Isolation and characterization of the signal recognition particle receptor. *J Cell Biol*. 95:470-477.

Gingras, A.-C., M. Gstaiger, B. Raught, and R. Aebersold. 2007. Analysis of protein complexes using mass spectrometry. *Nat Rev Mol Cell Bio*. 8:645-654.

Gohlke, U., L. Pullan, C.A. McDevitt, I. Porcelli, E. De Leeuw, T. Palmer, H.R. Saibil, and B.C. Berks. 2005. The TatA component of the twin-arginine protein transport system forms channel complexes of variable diameter. *Proc Natl Acad Sci USA*. 102:1048210486.

Goodsell, D.S., and A.J. Olson. 2000. Structural symmetry and protein function. *Annu Rev Biophys Biomol Struct*. 29:105-153.

Gross, J., and D. Bhattacharya. 2009. Mitochondrial and plastid evolution in eukaryotes: an outsiders' perspective. *Nat Rev Genet*. 10:495-505.

Gérard, F., and K. Cline. 2006. Efficient twin arginine translocation (Tat) pathway transport of a precursor protein covalently anchored to its initial cpTatC binding site. *J Biol Chem*. 281:6130-6135.

Gérard, F., and K. Cline. 2007. The thylakoid proton gradient promotes an advanced stage of signal peptide binding deep within the Tat pathway receptor complex. *J Biol Chem*. 282:5263-5272.

Hagan, C.L., T.J. Silhavy, and D.E. Kahne. 2010. β-barrel membrane protein assembly by the Bam complex. *Annu Rev Biochem*:1-22.

Hartl, F.U., B. Schmidt, E. Wachter, H. Weiss, and W. Neupert. 1986. Transport into mitochondria and intramitochondrial sorting of the Fe/S protein of ubiquinol-cytochrome c reductase. *Cell*. 47:939-951.

Hell, K., W. Neupert, and R.A. Stuart. 2001. Oxa1p acts as a general membrane insertion machinery for proteins encoded by mitochondrial DNA. *EMBO J*. 20:1281-1288.

Henry, R., R. Goforth, and D. Schunemann. 2007. Chloroplast SRP/FtsY and Alb3 in protein integration into the thylakoid membrane. *In* The enzymes, molecular machines involved in protein transport across cellular membranes. Vol. 25. R.E. Dalbey, C.M. Koehler, and F. Tamanoi, editors. Elsevier, London:. 493-521.

Heuberger, E.H.M.L., L.M. Veenhoff, R.H. Duurkens, R.H.E. Friesen, and B. Poolman. 2002. Oligomeric state of membrane transport proteins analyzed by blue native electrophoresis and analytical ultracentrifugation. *J Mol Biol*. 317:591-600.

Hinnah, S.C., K. Hill, R. Wagner, T. Schlicher, and J. Soll. 1997. Reconstitution of a chloroplast protein import channel. *EMBO J*. 16:7351-7360.

Hinnah, S.C., R. Wagner, N. Sveshnikova, R. Harrer, and J. Soll. 2002. The chloroplast protein import channel Toc75: pore properties and interaction with transit peptides. *Biophys J*. 83:899-911.

Hoepfner, D., D. Schildknegt, I. Braakman, P. Philippsen, and H.F. Tabak. 2005. Contribution of the endoplasmic reticulum to peroxisome formation. *Cell*. 122:85-95.

Inaba, T., M. Li, M. Alvarez-Huerta, F. Kessler, and D.J. Schnell. 2003. atTic110 functions as a scaffold for coordinating the stromal events of protein import into chloroplasts. *J Biol Chem*. 278:38617-38627.

Itoh, R., and Y. Fujiki. 2006. Functional domains and dynamic assembly of the peroxin Pex14p, the entry site of matrix proteins. *J Biol Chem*. 281:10196-10205.

Jack, R.L., F. Sargent, B.C. Berks, G. Sawers, and T. Palmer. 2001. Constitutive expression of Escherichia coli tat genes indicates an important role for the twin-arginine translocase during aerobic and anaerobic growth. *J Bacteriol*. 183:1801-1804.

Jakob, M., S. Kaiser, M. Gutensohn, P. Hanner, and R.B. Klösgen. 2009. Tat subunit stoichiometry in Arabidopsis thaliana challenges the proposed function of TatA as the translocation pore. *Biochim Biophys Acta*. 1793:388-394.

Jarvis, P., and C. Robinson. 2004. Mechanisms of protein import and routing in chloroplasts. *Curr Biol*. 14:1064-1077.

Jones, S., and J. Thoronton. 1996. Principles of protein-protein interactions. *Proc Natl Acad Sci USA*. 93:13-20.

Joo, C., H. Balci, Y. Ishitsuka, C. Buranachai, and T. Ha. 2010. Advances in single-molecule fluorescence methods for molecular biology. *Annu Rev Biochem*. 77:51-76.

Keegstra, K., and K. Cline. 1999. Protein import and routing systems of chloroplasts. *Plant Cell*. 11:557-570.

Kessler, F., G. Blobel, H. Patel, and D.J. Schnell. 1994. Identification of two GTP-binding proteins in the chloroplast protein import machinery. *Science*. 266:1035-1039.

Kikuchi, S., T. Hirohashi, and M. Nakai. 2006. Characterization of the preprotein translocon at the outer envelope membrane of chloroplasts by blue native PAGE. *Plant Cell Physiol*. 47:363-371.

Kikuchi, S., M. Oishi, Y. Hirabayashi, D.W. Lee, I. Hwang, and M. Nakai. 2009. A 1-megadalton translocation complex containing Tic20 and Tic21 mediates chloroplast protein import at the inner envelope membrane. *Plant cell*. 21:1781-1797.

Kohler, R., D. Boehringer, B. Greber, R. Bingel-Erlenmeyer, I. Collinson, C. Schaffitzel, and N. Ban. 2009. YidC and Oxa1 form dimeric insertion pores on the translating ribosome. *Mol Cell*. 34:344-353.

Komiya, T., S. Rospert, C. Koehler, R. Looser, G. Schatz, and K. Mihara. 1998. Interaction of mitochondrial targeting signals with acidic receptor domains along the protein import pathway: evidence for the 'acid chain' hypothesis. *EMBO J*. 17:3886-3898.

Kouranov, A., X. Chen, B. Fuks, and D.J. Schnell. 1998. Tic20 and Tic22 are new components of the protein import apparatus at the chloroplast inner envelope membrane. *J Cell Biol*. 143:991-1002.

Kunkele, K.-P., S. Heins, M. Dembowski, F.E. Nargang, R. Benz, M. Thieffry, J. Walz, R. Lill, S. Nussberger, and W. Neupert. 1998. The preprotein translocation channel of the outer membrane of mitochondria. *Cell*. 93:1009-1019.

Leake, M.C., N.P. Greene, R.M. Godun, T. Granjon, G. Buchanan, S. Chen, R.M. Berry, T. Palmer, and B.C. Berks. 2008. Variable stoichiometry of the TatA component of the twin arginine protein transport system observed by in vivo single-molecule imaging. *Proc Natl Acad Sci USA*. 105.

Lee, P.A., D. Tullman-Ercek, and G. Georgiou. 2006. The bacterial twin-arginine translocation pathway. *Annu Rev Microbiol*:373-395.

Li, H.-M., and C.-C. Chiu. 2010. Protein transport into chloroplasts. *Annu Rev Plant Biol*. 61:157-180.

Liang, F.C., U.K. Bageshwar, and S.M. Musser. 2009. Bacterial Sec protein transport is rate-limited by precursor length: a single turnover study. *Mol Biol Cell*. 20:4256.

Luirink, J., and I. Sinning. 2004. SRP-mediated protein targeting: structure and function revisited. *Biochim Biophys Acta*. 1694:17-35.

Ma, C., G. Agrawal, and S. Subramani. 2011. Peroxisome assembly: matrix and membrane protein biogenesis. *J Cell Biol*. 193:7-16.

Ma, X., and K. Cline. 2000. Precursors bind to specific sites on thylakoid membranes prior to transport on the ΔpH protein translocation system. *J Biol Chem*. 275:10016-10022.

Ma, X., and K. Cline. 2010. Multiple precursor proteins bind individual Tat receptor complexes and are collectively transported. *EMBO J*. 29.

Martin, J.R., J.H. Harwood, M. McCaffery, D.E. Fernandez, and K. Cline. 2009. Localization and integration of thylakoid protein translocase subunit cpTatC. *Plant J*. 58:831-842.

Meinecke, M., C. Cizmowski, W. Schliebs, V. Krüger, S. Beck, R. Wagner, and R. Erdmann. 2010. The peroxisomal importomer constitutes a large and highly dynamic pore. *Nat Cell Biol*. 12:273-277.

Meng, G., R. Fronzes, V. Chandran, H. Remaut, and G. Waksman. 2009. Protein oligomerization in the bacterial outer membrane. *Mol Membr Biol*. 26:136-145.

Mori, H., and K. Cline. 2002. A twin arginine signal peptide and the pH gradient trigger reversible assembly of the thylakoid ΔpH/Tat translocase. *J Cell Biol*. 157:205-210.

Mori, H., E. Summer, and K. Cline. 2001. Chloroplast TatC plays a direct role in thylakoid ΔpH-dependent protein transport. *FEBS Lett*. 501:65-68.

Moro, F., C. Sirrenberg, H.C. Schneider, W. Neupert, and M. Brunner. 1999. The TIM17/23 preprotein translocase of mitochondria: composition and function in protein transport into the matrix. *EMBO J*. 18:3667-3675.

Ménétret, J.-F., R.S. Hegde, S.U. Heinrich, P. Chandramouli, S.J. Ludtke, T.A. Rapoport, and C.W. Akey. 2005. Architecture of the ribosome-channel complex derived from native membranes. *J Mol Biol*. 348:445-457.

Müller, M., and R.B. Klösgen. 2005. The Tat pathway in bacteria and chloroplasts. *Mol Membr Biol*. 22:113-121.

Neupert, W., and J.M. Herrmann. 2007. Translocation of proteins into mitochondria. *Annu Rev Biochem*. 76:723-749.

Nielsen, E., M. Akita, J. Davila-Aponte, and K. Keegstra. 1997. Stable association of chloroplastic precursors with protein translocation complexes that contain proteins from both envelope membranes and a stromal Hsp100 molecular chaperone. *EMBO J*. 16:935-946.

Oliveira, M.E., A.M. Gouveia, R.A. Pinto, C. Sá-Miranda, and J.E. Azevedo. 2003. The energetics of Pex5p-mediated peroxisomal protein import. *J Biol Chem*. 278:39483-39488.

Osborne, A.R., and T.A. Rapoport. 2007. Protein translocation is mediated by oligomers of the SecY complex with one SecY copy forming the channel. *Cell*. 129:97-110.

Osborne, A.R., T.A. Rapoport, and B. van den Berg. 2005. Protein translocation by the Sec61/SecY channel. *Annu Rev Cell Dev Bi*. 21:529-550.

Panzner, S., L. Dreier, E. Hartmann, S. Kostka, and T.A. Rapoport. 1995. Posttranslational protein transport in yeast reconstituted with a purified complex of Sec proteins and Kar2p. *Cell*. 81:561-570.

Paschen, S.A., T. Waizenegger, T. Stan, M. Preuss, M. Cyrklaff, K. Hell, D. Rapaport, and W. Neupert. 2003. Evolutionary conservation of biogenesis of β-barrel membrane proteins. *Nature*. 426:862-866.

Patrick, T.D., C.E. Lewer, and V.M. Pain. 1989. Preparation and characterization of cell-free protein synthesis systems from oocytes and eggs of Xenopus laevis. *Development*. 106:1-9.

Pfeffer, S.R., and J.E. Rothman. 1987. Biosynthetic protein transport and sorting by the endoplasmic reticulum and Golgi. *Annu Rev Biochem*. 56:829-852.

Platta, H.W., and R. Erdmann. 2007. Peroxisomal dynamics. *Trends Cell Biol*. 17:474-484.

Platta, H.W., S. Grunau, K. Rosenkranz, W. Girzalsky, and R. Erdmann. 2005. Functional role of the AAA peroxins in dislocation of the cycling PTS1 receptor back to the cytosol. *Nat Cell Biol*. 7:817-822.

Pohlschröder, M., E. Hartmann, N.J. Hand, K. Dilks, and A. Haddad. 2005. Diversity and evolution of protein translocation. *Annu Rev Microbiol*. 59:91-111.

Purdue, P.E., X. Yang, and P.B. Lazarow. 1998. Pex18p and Pex21p, a novel pair of related peroxins essential for peroxisomal targeting by the PTS2 pathway. *J Cell Biol*. 143:1859-1869.

Rapoport, T.A. 2007. Protein translocation across the eukaryotic endoplasmic reticulum and bacterial plasma membranes. *Nature*. 450:663-669.

Reed, J., K. Cline, L. Stephens, K. Bacot, and P. Viitanen. 1990. Early events in the import/assembly pathway of an integral thylakoid protein. *Eur J Biochem*. 194:33-42.

Rehling, P., K. Model, K. Brandner, P. Kovermann, A. Sickmann, H.E. Meyer, W. Kühlbrandt, R. Wagner, K.N. Truscott, and N. Pfanner. 2003. Protein insertion into the mitochondrial inner membrane by a twin-pore translocase. *Science*. 299:1747-1751.

Richter, S., and G.K. Lamppa. 1998. A chloroplast processing enzyme functions as the general stromal processing peptidase. *Proc Natl Acad Sci USA*. 95:7463-7468.

Robert, V., E.B. Volokhina, F. Senf, M.P. Bos, P. Van Gelder, and J. Tommassen. 2006. Assembly factor Omp85 recognizes its outer membrane protein substrates by a species-specific C-terminal motif. *PLoS Biology*. 4:e377.

Saier, M.H. 2000. Families of proteins forming transmembrane channels. *J Membrane Biol*. 175:165-180.

Saier, M.H. 2003. Tracing pathways of transport protein evolution. *Mol Microbiol*. 48:1145-1156.

Sargent, F., B.C. Berks, and T. Palmer. 2006. Pathfinders and trailblazers: a prokaryotic targeting system for transport of folded proteins. *FEMS Microbiol Lett*. 254:198-207.

Schleiff, E., and T. Becker. 2010. Common ground for protein translocation: access control for mitochondria and chloroplasts. *Nat Rev Mol Cell Bio*. 12:48-59.

Schleiff, E., J. Soll, M. Küchler, W. Kühlbrandt, and R. Harrer. 2003. Characterization of the translocon of the outer envelope of chloroplasts. *J Cell Biol*. 160:541-551.

Schliebs, W., J. Saidowsky, B. Agianian, G. Dodt, F.W. Herberg, and W.H. Kunau. 1999. Recombinant human peroxisomal targeting signal receptor PEX5. Structural basis for interaction of PEX5 with PEX14. *J Biol Chem*. 274:5666-5673.

Schnell, D.J., F. Kessler, and G. Blobel. 1994. Isolation of components of the chloroplast protein import machinery. *Science*. 266:1007-1012.

Shi, L.-X., and S.M. Theg. 2010. A stromal heat shock protein 70 system functions in protein import into chloroplasts in the moss Physcomitrella patens. *Plant cell*. 22:205-220.

Shiozawa, K., P.V. Konarev, C. Neufeld, M. Wilmanns, and D.I. Svergun. 2009. Solution structure of human Pex5.Pex14.PTS1 protein complexes obtained by small angle X-ray scattering. *J Biol Chem*. 284:25334-25342.

Stanley, N.R., T. Palmer, and B.C. Berks. 2000. The twin arginine consensus motif of Tat signal peptides is involved in Sec-independent protein targeting in Escherichia coli. *J Biol Chem*. 275:11591-11596.

Stanley, W.A., and M. Wilmanns. 2006. Dynamic architecture of the peroxisomal import receptor Pex5p. *Biochim Biophys Acta*. 1763:1592-1598.

Su, P.-H., and H.-M. Li. 2008. Arabidopsis stromal 70-kD heat shock proteins are essential for plant development and important for thermotolerance of germinating seeds. *Plant Physiol*. 146:1231-1241.

Sveshnikova, N., R. Grimm, J. Soll, and E. Schleiff. 2000. Topology studies of the chloroplast protein import channel Toc75. *Biol Chem*. 381:687-693.

Tarry, M.J., E. Schäfer, S. Chen, G. Buchanan, N.P. Greene, S.M. Lea, T. Palmer, H.R. Saibil, and B.C. Berks. 2009. Structural analysis of substrate binding by the TatBC component of the twin-arginine protein transport system. *Proc Natl Acad Sci USA*. 106:13284-13289.

Truscott, K.N., P. Kovermann, a. Geissler, a. Merlin, M. Meijer, a.J. Driessen, J. Rassow, N. Pfanner, and R. Wagner. 2001. A presequence- and voltage-sensitive channel of the mitochondrial preprotein translocase formed by Tim23. *Nat Struct Biol*. 8:1074-1082.

van Loon, A.P.G.M., A.W. Brändli, and G. Schatz. 1986. The presequences of two imported mitochondrial proteins contain information for intracellular and intramitochondrial sorting. *Cell*. 44:801-812.

Webb, C.T., M.A. Gorman, M. Lazarou, M.T. Ryan, and J.M. Gulbis. 2006. Crystal structure of the mitochondrial chaperone TIM9.10 reveals a six-bladed alpha-propeller. *Mol Cell*. 21:123-133.

Wickner, W., and R. Schekman. 2005. Protein translocation across biological membranes. *Science*. 310:1452-1456.

Wiedemann, N., V. Kozjak, A. Chacinska, B. Schönfisch, S. Rospert, M.T. Ryan, N. Pfanner, and C. Meisinger. 2003. Machinery for protein sorting and assembly in the mitochondrial outer membrane. *Nature*. 424:565-571.

Young, M.E., K. Keegstra, and J.E. Froehlich. 1999. GTP promotes the formation of early-import intermediates but is not required during the translocation step of protein import into chloroplasts. *Plant Physiol*. 121:237-244.

BIOGRAPHICAL SKETCH

Jose Celedon developed an early interest in biology that probably started in his frequent family hiking trips in the Andes, Chile. This, together with multiple summers working at his uncle's farm made him decide to study Agriculture Engineering at the University of Chile in Santiago. After 5 years of course work and a year working in his thesis, he graduated with honors and started working as a research assistant with Professor Fernando Santibanhez in crop computer models and geographical information systems at University of Chile.

Jose decided next to get some experience working in a plant physiology lab, and joined Professor Raul Ferreyra's group at the National Research Institute for Agriculture, Chile. He was part of a project to study tree water stress that involved field and laboratory experiments to understand plant's responses to drought and flooding. This project had scientific as well as economic impact since the plant used in the experiments, Avocado trees, is an important crop in Chile's agriculture industry.

After learning the importance and need for research in his country, Jose obtained a Fulbright scholarship to come to the United States and pursue a PhD. He chose to work in chloroplast protein transport in the laboratory of Dr. Kenneth Cline at the Department of Horticultural Sciences, University of Florida. This training and experience in the field of plant molecular biology and biochemistry would complement his previous work in plant physiology and allow him to do deeper and more significant research in plant related issues.